Bulletin of Mathematical Biology (2025) 87:87
https://doi.org/10.1007/s11538-025-01469-3

Society for Mathematical Biology

ORIGINAL ARTICLE

Transmission of Multiple Pathogens Across Species

Clotilde Djuikem[1] · **Julien Arino**[1]

Received: 29 May 2024 / Accepted: 21 May 2025

Abstract
We analyse a model that describes the propagation of many pathogens within and between many species. A branching process approximation is used to compute the probability of disease outbreaks. Special cases of aquatic environments with two host species and one or two pathogens are considered both analytically and computationally.

Keywords Multiple species–multiple pathogens · Branching process approximation · Introductions

1 Introduction

The ranges of species are continuously changing (Kirkpatrick and Barton 1997; Sexton et al. 2009). However, the process has accelerated in recent years because of climate change (Atkins and Travis 2010; Parmesan 2006). Regardless of what is driving their evolution, a consequence of the modification of ranges is more frequent interactions between species that did not use to interact or interacted quite infrequently.

This has a wide variety of consequences. Competition for resources is modified if an invading species is, for instance, using the same resource as a resident one. This is thought to be one of the main drivers of species evolution (Phillips et al. 2010). Range shifting can also lead to the introduction into ecosystems of pathogens from which they were absent, when species whose range now includes these ecosystems become more frequent there (Carlson et al. 2022). Introductions of pathogens due to range shifting is also very similar to what happens when human populations encroach into the ranges of species (Ellwanger and Chies 2021), which has led to an increasing number of spillover events (Meadows et al. 2023).

In both cases, some of the populations involved may be hosts to a wide variety of pathogens. Understanding a situation with different pathogens and different species is therefore important.

The specific motivation for the present work comes from the observation that salmonids are observed increasingly frequently the Mackenzie River, in the west-

✉ Clotilde Djuikem
clotilde.djuikem@umanitoba.ca

[1] University of Manitoba, Winnipeg, Canada

Published online: 28 May 2025

ern Canadian arctic. Of interest to collaborators from Fisheries and Oceans Canada (see *Acknowledgments*) is the fact that these vagrant salmon species spend most of their lives in distant ecosystems, where they can acquire pathogens that are, to this point, mostly absent from the Mackenzie River aquatic ecosystem. When they are collocated in that ecosystem, those vagrant species can in turn transmit those novel pathogens to resident species.

While pathogens abound in terrestrial ecosystems, the situation is even more pronounced in aquatic ecosystems, where numerous pathogens are present (Bergh et al. 1989; Wommack and Colwell 2000; Wyn-Jones and Sellwood 2001). Viruses, for instance, are estimated to be the most abundant "lifeforms" in the oceans, representing over 90% of the nucleic-acid-containing particles and about 5% of the biomass there (Suttle 2007). Many aquatic pathogens infect fish species, so that the invading species mentioned earlier may be coming into contact with a wide variety of pathogens prior to their entering a novel ecosystem.

Our aim is therefore to establish models to help understand the introduction of pathogens in species from which they were absent up to that point, when these species come into contact with other species potentially bearing the pathogen. The model in this paper is a simplified model and serves to set the general setting in which we operate. We use a simple SLIR model, whose dynamics in a single location and single population is well understood, but assume that there are multiple species of hosts as well as multiple pathogen species. We also assume that there is no coinfection with multiple pathogens.

The article is organised as follows. In Sect. 2, an ordinary differential equations (ODE) multi-species epidemiological model is introduced, followed by its continuous time Markov chain (CTMC) equivalent. The section also presents an analysis of both the ODE and CTMC models, the latter using a branching process approximation to compute the probability of a disease outbreak. Section 3 focuses on the case of two species and one pathogen, with example scenarios corresponding to three different fish viruses investigated numerically, as well as a particular case focusing on introduction of a pathogen by a species in which it is endemic. In Sect. 4, the case of two species and two pathogens is discussed.

2 The General Model

Consider P populations. These populations could be the same or different species, the important feature being that they be distinguishable according to some criterion. In the sequel, we use both terms, *species* and *population*, interchangeably. Within and between these populations, V pathogens can propagate. Specifically, each population is described by an SLIR epidemic model, where susceptible individuals in a given population can become infected by any of the V viruses if they come into contact with an individual infected by it, regardless of the population that individual belongs to.

Further, we assume that coinfection does not occur, i.e., once infected by a given pathogen, an individual cannot acquire infection from another pathogen. This is a strong assumption. Coinfections are known to occur frequently both in fish species (Kotob et al. 2017) and more generally (since our model could be applied to other situ-

ations) Karvonen et al. (2019). However, as noted by Kotob et al. (2017), coinfections are poorly understood and the data is scarce for coinfections in animal species. This true also in humans; see, e.g., Klein et al. (2016). Some pathogens interact synergistically, others are antagonistic, so it is not clear *a priori* whether being infected with one pathogen facilitates or hinders infection with another. As a consequence and as a first approximation, we make this assumption, meaning that in a way, we are focusing on the primary infection.

Another strong assumption of the model is that infection with one pathogen confers, upon recovery, permanent immunity to all pathogens. This is, of course, an oversimplification, but it is applicable for example in situations where pathogens are antigenically close and natural infection induces broad and long-lived immune responses Krammer (2019). It is also important to bear in mind that, depending on the species under consideration, recovery from infection with some pathogens may take a long time or even never occur, so that an individual may remain infectious and potentially immune to infection with another pathogen until they die.

2.1 Formulation of the Deterministic Model

For $p = 1, \ldots, P$, denote S_p the number of individuals susceptible to infection in the pth population. Individuals of species p may become infected by any of the V pathogens present when they come across an individual infectious with that pathogen. The parameter describing the rate at which contacts between a susceptible from species p and an infectious individual from species $q = 1, \ldots, P$ infected with pathogen $v = 1, \ldots, V$, results in new infections, is β_{pqv}, i.e., in words, the parameter β has indices

$$\beta_{\text{who becomes infected, who infects, with which pathogen}}.$$

Incidence is assumed to be mass action.

Upon infection, individuals of species $p = 1, \ldots, P$ infected by pathogen $v = 1, \ldots, V$ become latently infected, with numbers denoted L_{pv}. We do not consider coinfection with multiple pathogens; once an individual is contaminated with any of the viruses, they cannot become infected by any other pathogen.

After an incubation period of mean duration $1/\varepsilon_{pv}$ time units, individuals of species p infected with pathogen v become infectious to others. The number of such infectious individuals is denoted I_{pv}. Finally, after an average $1/\gamma_{pv}$ time units spent infectious with the pathogen, individuals recover and move to the R_p compartment. Note that the recovery rate may be very small or even zero in the case of some pathogens, with individuals remaining infectious until they die. At this point, the pathogen they were infected with is ignored as it is not relevant to the problem under consideration. Regarding species demography, birth into population $p = 1, \ldots, P$ occurs at the fixed rate b_p, while death occurs in all compartments at the *per capita* rate d_p.

Taking all this into account, we have a group model, with dynamics of the different states governed for population $p = 1, \ldots P$ and pathogen $v = 1, \ldots, V$ by the following ordinary differential equations:

Table 1 State variables and their meaning

Variable	Meaning
S_p	Susceptible individual in population p
L_{pv}	Latent individual in population p infected by virus v
I_{pv}	Individual in population p infectious with virus v
R_p	Recovered individual in population p

$$\dot{S}_p = b_p - \left(\sum_{q=1}^{P} \sum_{v=1}^{V} \beta_{pqv} I_{qv} + d_p \right) S_p, \tag{1a}$$

$$\dot{L}_{pv} = \sum_{q=1}^{P} \beta_{pqv} I_{qv} S_p - (\varepsilon_{pv} + d_p) L_{pv}, \tag{1b}$$

$$\dot{I}_{pv} = \varepsilon_{pv} L_{pv} - (\gamma_{pv} + d_p) I_{pv}, \tag{1c}$$

$$\dot{R}_p = \sum_{v=1}^{V} \gamma_{pv} I_{pv} - d_p R_p. \tag{1d}$$

System (1) is considered with nonnegative initial conditions. To avoid a trivial case, it is assumed that $L_{pv} + I_{pv} > 0$ for at least one $(p, v) \in \{1, \ldots, P\} \times \{1, \ldots, V\}$. The total size of each population p for $i = 1, \ldots, P$ is given by:

$$N_p = S_p + \sum_{v=1}^{V} L_{pv} + \sum_{v=1}^{V} I_{pv} + R_p. \tag{2}$$

2.2 Notation

Equations (1b) and (1c) involve two different indices. Analysis of the system often requires to list these indices. To simplify presentation, for given symbols X and Y, we use the notation

$$\begin{aligned}
&[\![X_p]\!] = X_1, \ldots, X_P, \\
&[\![X_{pv}]\!] = X_{11}, X_{12}, \ldots, X_{1V}, X_{21}, X_{22}, \ldots, X_{2V}, \ldots, X_{P1}, X_{P2}, \ldots, X_{PV}
\end{aligned}$$

and

$$\begin{aligned}
[\![X_{pv} + Y_p]\!] = {} & X_{11} + Y_1, X_{12} + Y_1, \ldots, X_{1V} + Y_1, \\
& X_{21} + Y_2, X_{22} + Y_2, \ldots, X_{2V} + Y_2, \ldots, \\
& X_{P1} + Y_P, X_{P2} + Y_P, \ldots, X_{PV} + Y_P.
\end{aligned}$$

Thus, when multiple indices are present, we present indices as would the row-first enumeration of indices of the entries of a $P \times V$ matrix. Note that the assumption is that indices p and v are reserved, respectively, for population and virus species indices and therefore run in $1, \ldots, P$ and $1, \ldots, V$.

2.3 Basic Analysis of the Deterministic Model

The disease-free equilibrium (DFE) of system (1) is

$$\boldsymbol{E}_0^{(1)} = \left([\![S_p^0]\!], 0_{\mathbb{R}^{P(2V+1)}} \right), \tag{3}$$

where $S_p^0 = b_p/d_p$ for $p = 1, \ldots, P$. Note that for equilibria as well as for the basic reproduction number, we use a superscript to refer to the specific form of the system that is being considered.

To determine the matrices used in the computation of the basic reproduction number using the next generation matrix method of van den Driessche and Watmough (2002), order infected variables by type: $[\![L_{pv}]\!], [\![I_{pv}]\!]$. Then the nonnegative $2PV \times 2PV$-matrix $\mathbf{G}$ has block form

$$\mathbf{G} = \begin{bmatrix} 0 & \mathbf{G}_{12} \\ 0 & 0 \end{bmatrix}, \tag{4}$$

where the $PV \times PV$-matrix $\mathbf{G}_{12}$ is itself a block matrix, with each $V \times V$ sized block taking the form, for $p, q \in \{1, \ldots, P\}$,

$$\mathbf{G}_{12}^{pq} = S_p^0 \mathsf{diag}(\beta_{pq1}, \ldots, \beta_{pqV}). \tag{5}$$

The matrix $\mathbf{W}$ is a nonnegative $2PV \times 2PV$-matrix and has block form

$$\mathbf{W} = \begin{bmatrix} \mathbf{W}_{11} & \mathbf{0} \\ -\mathbf{W}_{21} & \mathbf{W}_{22} \end{bmatrix}, \tag{6}$$

with the $PV \times PV$-sized block taking the form

$$\mathbf{W}_{11} = \mathsf{diag}([\![\varepsilon_{pv} + d_p]\!]), \mathbf{W}_{21} = \mathsf{diag}([\![\varepsilon_{pv}]\!]) \text{ and } \mathbf{W}_{22} = \mathsf{diag}([\![\gamma_{pv} + d_p]\!]). \tag{7}$$

The basic reproduction number of (1) is then the spectral radius of $\mathbf{G}\mathbf{W}^{-1}$ and is given by $\mathcal{R}_0^{(1)} = \rho(\mathbf{G}\mathbf{W}^{-1})$. Since $\mathbf{W}$ is block lower triangular,

$$\mathbf{W}^{-1} = \begin{bmatrix} \mathbf{W}_{11}^{-1} & \mathbf{0} \\ \mathbf{W}_{22}^{-1}\mathbf{W}_{21}\mathbf{W}_{11}^{-1} & \mathbf{W}_{22}^{-1} \end{bmatrix},$$

whence, from the form of $\mathbf{G}$, we obtain

$$\mathcal{R}_0^{(1)} = \rho(\mathbf{G}_{12}\mathbf{W}_{22}^{-1}\mathbf{W}_{21}\mathbf{W}_{11}^{-1}).$$

The matrices (7) are diagonal and the structure of $\mathbf{G}_{12}$ is relatively simple; it is therefore possible to further simplify the expression above. We obtain

$$\mathcal{R}_0^{(1)} = \max_{v=1,\dots,V} \mathcal{R}_0^v, \tag{8}$$

where

$$\mathcal{R}_0^v = \rho(\mathcal{B}_v),$$

is the basic reproduction number of virus $v = 1, \dots, V$ and $\mathcal{B}_v$ is a $P \times P$-matrix defined as

$$\mathcal{B}_v = [\mathcal{B}_{pqv}]_{pq}, \tag{9}$$

where $\mathcal{B}_{pqv}$ denotes the element in the p-th row and q-th column of the matrix $\mathcal{B}_v$ and is given by

$$\mathcal{B}_{pqv} = \frac{\beta_{pqv}\varepsilon_{qv}S_p^0}{(\varepsilon_{qv} + d_q)(\gamma_{qv} + d_q)},$$

for $p, q = 1, \dots, P,\ v = 1, \dots, V$.

From (van den Driessche and Watmough (2002),,Theorem 2) we deduce the following result concerning the local asymptotic stability of the disease-free equilibrium $\boldsymbol{E}_0^{(1)}$.

Lemma 1 *The disease-free equilibrium $\boldsymbol{E}_0^{(1)}$ of (1) is locally asymptotically stable if $\mathcal{R}_0^{(1)} < 1$ and unstable if $\mathcal{R}_0^{(1)} > 1$.*

Remark that in the absence of interaction between the populations, i.e., when $\beta_{p\ell v} = 0$ if $p \neq \ell$, the basic reproduction number in each population $p = 1, \dots, P$ is given by

$$\mathcal{R}_{0p} = \max_{v=1,\dots,V}(\mathcal{R}_{0p}^v), \text{ where } \mathcal{R}_{0p}^v = \frac{\beta_{ppv}\varepsilon_{pv}S_p^0}{(\varepsilon_{pv} + d_p)(\gamma_{pv} + d_p)}. \tag{10}$$

Various forms of the reproduction numbers appear in the remainder of the text. To clarify, we list them here.

- $\mathcal{R}_{0p}$ denotes the basic reproduction number of species p in the presence of multiple pathogens V, excluding other species.
- $\mathcal{R}_{0p}^v$ denotes the basic reproduction number of species p in the presence of a single pathogen v, excluding other species.
- $\mathcal{R}_0^v$ denotes the basic reproduction number of a single pathogen v across P interacting species.
- $\mathcal{R}_0$ denotes the basic reproduction number of multiple pathogens V across multiple interacting species P, i.e, for the full (1).

Asymptotic stability is in fact global for a given pathogen when $\mathcal{R}_0 < 1$, as established in the following theorem.

Table 2 Events, transitions $\mathbf{k} \to \mathbf{j}$ and transition rates $\sigma(\mathbf{k}, \mathbf{j})$ of the general CTMC model (11)

Event	Transition	Transition rate
Birth of S_p	$S_p \to S_p + 1$	b_p
Natural death of S_p	$S_p \to S_p - 1$	$d_p S_p$
Natural death of L_{pv}	$L_{pv} \to L_{pv} - 1$	$d_p L_{pv}$
Natural death of I_{pv}	$I_{pv} \to I_{pv} - 1$	$d_p I_{pv}$
Natural death of R_p	$R_p \to R_p - 1$	$d_p R_p$
Infection of S_p by I_{qv}	$S_p \to S_p - 1, L_{pv} \to L_{pv} + 1$	$\beta_{pqv} I_{qv} S_p$
End of incubation of L_{pv}	$L_{pv} \to L_{pv} - 1, I_{pv} \to I_{pv} + 1$	$\varepsilon_{pv} L_{pv}$
Recovery of I_{pv}	$I_{pv} \to I_{pv} - 1, R_p \to R_p + 1$	$\gamma_{pv} I_{pv}$

Theorem 2 *If $\mathcal{R}_0^{(1)} < 1$, then the DFE $\boldsymbol{E}_0^{(1)}$ is globally asymptotically stable (GAS) in Ω, where*

$$\Omega = \Bigg\{ ([\![S_p]\!], [\![L_{pv}]\!], [\![I_{pv}]\!], [\![R_p]\!]) \in \mathbb{R}^{2P(V+1)} : \\ N_p = S_P + \sum_{v=1}^{V} (L_{pv} + I_{pv}) + R_p \leq \frac{b_p}{d_p}; \quad p = 1, \ldots, P \Bigg\}.$$

This result is proved in Appendix B.

2.4 The Continuous time Markov Chain Model

We now consider a continuous time Markov chain (CTMC) related to the ODE system (1). CTMCs allow to explore various scenarios that the deterministic models cannot capture. In particular, CTMCs of the type used here have discrete state variables, thereby allowing transitions toward a state where the disease is eradicated. In ODE models, such states are typically approached only as limits, which leads to implausible situations (Fowler 2021).

Let T denote the set of all finite-dimensional vectors whose components are non-negative integers. The CTMC model related to the deterministic model (1) then takes the form,

$$\mathbf{X}_t = \left([\![S_p(t)]\!], [\![L_{pv}(t)]\!], [\![I_{pv}(t)]\!], [\![R_p(t)]\!] \right), \quad t \in \mathbb{R}_+, \tag{11a}$$

where each element of the vector is a collection of discrete random variables that take values in T and where the time between events is exponentially distributed (Allen 2010). The process is time-homogeneous as the rates in the ODE are constants, so the CTMC is characterised by transition probabilities from state $\mathbf{k}$ to state $\mathbf{j}$,

$$\mathbb{P}(\mathbf{X}(t + \Delta t) = \mathbf{j} \mid \mathbf{X}(t) = \mathbf{k}) = \sigma(\mathbf{k}, \mathbf{j}), \tag{11b}$$

with transition rates $\sigma(\mathbf{k}, \mathbf{j})$ given in Table 2.

Note that the β_{pqv} used in the CTMC and the ODE do not have the same units. However, since the total population N_p of species p is asymptotically constant in the ODE (1), the transmission parameter β_{pqv} in the ODE can be written as $\beta_{pqv} = \tilde{\beta}_{pqv}/N_p$. In this sense, using mass action or proportional incidence makes no difference except in the units and values of the transmission parameter.

2.5 Branching Process Approximation of the CTMC

We use a multitype branching process approximation (MBPA) to approximate the CTMC $\mathbf{X}_t$ near the disease-free equilibrium. This approximation allows to study the early phase of the epidemic, when most individuals are still susceptible, meaning that the infection process can be treated as being approximately linear. Indeed, by the scaling mentioned in Sect. 2.4, it can be assumed that transmission takes the form $\beta SI/N$ with $S \simeq N$ at the start of the outbreak.

Let $Z(t) = ([\![Z^{\ell}_{pv}(t)]\!], [\![Z^{i}_{pv}(t)]\!]) := [\![Z^{k}_{pv}(t)]\!]$ be a $2PV$-type branching process, where $Z^{k}_{pv}(t)$ denotes the number of individuals of type (k, p, v) at time t. Here, $k \in \{\ell, i\}$ refers to latent or infectious states, $p = 1, \ldots, P$ is the host species, and $v = 1, \ldots, V$ is the virus type. The set of all possible types (k, p, v) defines the structure of the multitype process.

Each individual of type (i, q, v), denoted I_{qv}, remains infectious for a time that follows an exponential distribution with parameter $d_q + \gamma_{qv}$. During its infectious period, it produces individuals of type (ℓ, p, v) at rate $\beta_{pqv} S^0_p$ for each $p = 1, \ldots, P$, where S^0_p denotes the initial number of susceptibles of species p. This transmission is independent from transmissions by other infectious individuals since almost all the population is susceptible. Each infectious individual then recovers with probability $\gamma_{qv}/(d_q + \gamma_{qv})$ or dies before recovering with probability $d_q/(d_q + \gamma_{qv})$.

In turn, each latent individual of type (ℓ, p, v), denoted L_{pv}, remains so for an exponentially distributed time with parameter $d_p + \varepsilon_{pv}$. Upon transition out of L_{pv}, it produces an individual of type (i, p, v) with probability $\varepsilon_{pv}/(d_p+\varepsilon_{pv})$, corresponding to the progression from the latent to the infectious state, or dies without producing infectious offspring with probability $d_p/(d_p + \varepsilon_{pv})$. All lifetimes, infection events, and transitions are assumed to be mutually independent across individuals.

The associated discrete-time multitype Galton-Watson (GW) process describes the evolution across successive generations: each infectious individual of type (i, q, v) produces, for each $p = 1, \ldots, P$, a number of latent individuals of type (ℓ, p, v) following a geometric distribution with parameter $\beta_{pqv} S^0_p / \left(d_q + \gamma_{qv} + \sum_{p=1}^{P} \beta_{pqv} S^0_p\right)$.

Having described the process, we now derive the probability generating function (p.g.f.) $F(t, \mathbf{u}) = [\![F^{k}_{pv}(\mathbf{u})]\!]$ for the full process using (Athreya and Ney (1972),Chapter V Sect. 1), with

$$F^{k}_{pv}(t, \mathbf{u}) = \mathbb{E}\left[\mathbf{u}^{Z(t)} \,\middle|\, Z(0) = e^{k}_{pv}\right], \tag{12}$$

where $\mathbb{E}$ is the expectation, e^{k}_{pv} is the standard unit vector corresponding to type (k, p, v) and $\mathbf{u} = ([\![u^{\ell}_{pv}]\!], [\![u^{i}_{pv}]\!]) := [\![u^{k}_{pv}]\!]$ is a vector with $u^{k}_{pv} \in [0, 1]$. The notation

$\mathbf{u}^{Z(t)}$ stands for the product

$$\mathbf{u}^{Z(t)} = \prod_{(k',p',v')} (u_{p'v'}^{k'})^{Z_{p'v'}^{k'}(t)}.$$

Using the branching property and standard results from the theory of branching processes (Athreya and Ney (1972),Chapter V Section 7.1), we obtain the backward Kolmogorov differential equation for all (k, p, v) types,

$$\frac{\partial}{\partial t} F_{pv}^{k}(t, \mathbf{u}) = \omega_{pv}^{k} \left[f_{pv}^{k}(F(t, \mathbf{u})) - F_{pv}^{k}(t, \mathbf{u}) \right], \tag{13}$$

with initial condition $[\![F_{pv}^{k}(0, \mathbf{u})]\!] = [\![u_{pv}^{k}]\!]$. Here, ω_{pv}^{k} is the parameter of the exponential distribution for the time that an individual spends as an (k, p, v)-type individual and $f_{pv}^{k}(F(t, \mathbf{u}))$ is the contribution of the offspring of (k, p, v)-type individuals to the generation of offspring.

The function $f_{pv}^{k}(\mathbf{u}) := f_{pv}^{k}(F(0, \mathbf{u}))$, which we call the *offspring generating function*, is the distribution of the number and types of first-generation offspring produced by a single individual of type (k, p, v) during its time as an (k, p, v)-type individual. Formally,

$$f_{pv}^{k}(\mathbf{u}) = \sum_{[\![r_{pv}^{k}]\!]=0}^{\infty} \mathbb{P}\left([\![r_{pv}^{k}]\!] \right) \prod_{(k',p',v')} (u_{p'v'}^{k'})^{r_{p'v'}^{k'}}, \tag{14}$$

where $\mathbb{P}([\![r_{pv}^{k}]\!])$ denotes the probability that an individual of type (k, p, v) produces $r_{p'v'}^{k'}$ individuals of type (k', p', v') during its time as an (k, p, v)-type individual.

Using the general form in (14) and using the infinitesimal transition rates of the CTMC near the disease-free equilibrium, assuming $S_p = S_p^0$ is constant, the offspring generating functions are given by

$$f_{pv}^{\ell}(\mathbf{u}) = \frac{\varepsilon_{pv} u_{pv}^{i} + d_p}{\varepsilon_{pv} + d_p}, \tag{15a}$$

$$f_{pv}^{i}(\mathbf{u}) = \frac{\left(\sum_{q=1}^{P} \beta_{qpv} S_q^0 u_{qv}^{\ell} \right) u_{pv}^{i} + \gamma_{pv} + d_p}{\Lambda_{pv}}, \tag{15b}$$

with

$$\Lambda_{pv} = \sum_{q=1}^{P} \beta_{pqv} S_q^0 + \gamma_{pv} + d_p.$$

The following result then holds, which is proved in Appendix C.

Theorem 3 *The multitype branching process is positive regular and nonsingular, the probabilities of extinction and outbreak in the multitype branching process with probability generating functions (15) are given by*

$$\mathbb{P}_{ext} = \prod_{p=1}^{P}\prod_{v=1}^{V}(z_{pv}^{\ell})^{\ell_{pv0}}(z_{pv}^{i})^{i_{pv0}} = \prod_{p=1}^{P}\prod_{v=1}^{V}\left(\frac{\varepsilon_{pv}z_{pv}^{i}+d_p}{\varepsilon_{pv}+d_p}\right)^{\ell_{pv0}}(z_{pv}^{i})^{i_{pv0}}, \tag{16a}$$

$$\mathbb{P}_{outbreak} = 1 - \mathbb{P}_{ext}, \tag{16b}$$

where

$$z := \left([\![z_{pv}^{\ell}]\!], [\![z_{pv}^{i}]\!]\right)$$

is a fixed point on $[0,1]^{2PV}$ *of the p.g.f. (15) and* $[\![L_{pv}(0)]\!] = [\![\ell_{pv0}]\!]$, $[\![I_{pv}(0)]\!] = [\![i_{pv0}]\!]$ *is the initial condition. Moreover, the following alternative holds:*

- *if* $\mathcal{R}_0^{(1)} \leq 1$, *then* $z = \mathbf{1}$, *i.e.,* $\mathbb{P}_{ext} = 1$;
- *if* $\mathcal{R}_0^{(1)} > 1$, *then additionally to* $z = \mathbf{1}$, *there is a unique vector* $\mathbf{0} < z < \mathbf{1}$ *such that* $\mathbf{F}(z) = z$.

In MBPA, processes either reach zero or approach infinity. The probability of extinction is interpreted in our model as the probability of a minor epidemic, while an outbreak is the establishment of the pathogen. However, once the number of infected individuals in the branching process reaches a certain level, it is no longer an accurate approximation of the epidemic, as the MBPA does not adequately represent dynamics far from the disease-free equilibrium.

3 Case of One Pathogen and Two Species

To get better insight into the behaviour of the system in a tractable case, we consider the case with $P = 2$ species and $V = 1$ pathogen. We first specialise the model and results of mathematical analysis to this special case (Sect. 3.1), then consider numerically four specific transmission scenarios, which we also summarise by indicating the type of propagation taking place between populations P_1 and P_2.

1. Pathogen propagation within and between species (Sect. 3.2, $P_1 \leftrightarrow P_2$).
2. The pathogen is transmitted to both species, but one species can only infect members of its species (Sect. 3.3, $P_1 \to P_2$, $P_2 \not\to P_1$).
3. Both species can acquire the pathogen, but one of the two species does not become a transmitter (Sect. 3.4, $P_1 \to P_2$, $P_2 \not\to$).
4. The pathogen is established at an endemic level in one species and is absent from the other species (Sect. 3.5, $P_1^{\star} \to P_2$).

3.1 The Models and Their Basic Analysis

Because $V = 1$, the second index of ε and γ and the third index of β always equals 1. To simplify notation, in the remainder of Sect. 3, we drop this superfluous index and write ε_p, γ_p and β_{pq}, for $p, q = 1, \ldots, P$.

3.1.1 The ODE Model When $P = 2$ and $V = 1$

Setting $P = 2$ and $V = 1$ in (1) gives

$$\dot{S}_1 = b_1 - \beta_{11} S_1 I_1 - \beta_{12} S_1 I_2 - d_1 S_1 \tag{17a}$$
$$\dot{L}_1 = \beta_{11} S_1 I_1 + \beta_{12} S_1 I_2 - (\varepsilon_1 + d_1) L_1 \tag{17b}$$
$$\dot{I}_1 = \varepsilon_1 L_1 - (\gamma_1 + d_1) I_1 \tag{17c}$$
$$\dot{R}_1 = \gamma_1 I_1 - d_1 R_1 \tag{17d}$$
$$\dot{S}_2 = b_2 - \beta_{21} S_2 I_1 - \beta_{22} S_2 I_2 - d_2 S_2 \tag{17e}$$
$$\dot{L}_2 = \beta_{21} S_2 I_1 + \beta_{22} S_2 I_2 - (\varepsilon_2 + d_2) L_2 \tag{17f}$$
$$\dot{I}_2 = \varepsilon_2 L_2 - (\gamma_2 + d_2) I_2 \tag{17g}$$
$$\dot{R}_2 = \gamma_2 I_2 - d_2 R_2, \tag{17h}$$

The system is considered with variables ordered as $S_1, S_2, L_1, L_2, I_1, I_2, R_1, R_2$. The analysis in Sect. 2.3 carries through, taking into account that since $V = 1$, a few adaptations of the terms and matrices defined there are required. The disease-free equilibrium (DFE) of (17) is

$$\boldsymbol{E}_0^{(17)} = \left([\![S_p^0]\!], \mathbf{0}_{\mathbb{R}^{3P}} \right) = \left(\frac{b_1}{d_1}, \frac{b_2}{d_2}, \mathbf{0}_{\mathbb{R}^6} \right), \tag{18}$$

infected variables are $[\![L_p]\!]$, $[\![I_p]\!]$, $P \times P$ matrix $\mathbf{G}_{12}$ is not a block matrix but instead has entry (p, q) equal to $S_p^0 \beta_{pq}$ and, since $P = 2$,

$$\mathbf{G}_{12} = \begin{pmatrix} \beta_{11} S_1^0 & \beta_{12} S_1^0 \\ \beta_{21} S_2^0 & \beta_{22} S_2^0 \end{pmatrix}.$$

Blocks in the matrix $\mathbf{W}$ take the form

$$\mathbf{W}_{11} = \mathsf{diag}([\![\varepsilon_p + d_p]\!]), \mathbf{W}_{21} = \mathsf{diag}([\![\varepsilon_p]\!]) \text{ and } \mathbf{W}_{22} = \mathsf{diag}([\![\gamma_p + d_p]\!]),$$

so that in the case $P = 2$ under consideration,

$$\mathbf{W} = \begin{pmatrix} \varepsilon_1 + d_1 & 0 & 0 & 0 \\ 0 & \varepsilon_2 + d_2 & 0 & 0 \\ -\varepsilon_1 & 0 & \gamma_1 + d_1 & 0 \\ 0 & -\varepsilon_2 & 0 & \gamma_2 + d_2 \end{pmatrix}.$$

Table 3 Reaction rates used to determine transition probabilities for 2-species and 1-pathogen CTMC model

Event ($p = 1, 2$)	Transition	Transition rates
Birth of S_p	$S_p \to S_p + 1$	b_p
Natural death of S_p	$S_p \to S_p - 1$	$d_p S_p$
Natural death of L_p	$L_p \to L_p - 1$	$d_p L_p$
Natural death of I_p	$I_p \to I_p - 1$	$d_p I_p$
Natural death of R_p	$R_p \to R_p - 1$	$d_p R_p$
Infection of S_p by I_q	$S_p \to S_p - 1, L_p \to L_p + 1$	$\beta_{pq} S_p I_q$
End of incubation of L_p	$L_p \to L_p - 1, I_p \to I_p + 1$	$\varepsilon_p L_p$
Recovery in I_p	$I_p \to I_p - 1, R_p \to R_p + 1$	$\gamma_p I_p$

It follows that the basic reproduction number of (17) is

$$\mathcal{R}_0^{(17)} = \frac{\beta_{11}\kappa_1 S_1^0 + \beta_{22}\kappa_2 S_2^0 + \sqrt{\left(\beta_{11}\kappa_1 S_1^0 - \beta_{22}\kappa_2 S_2^0\right)^2 + 4\beta_{12}\beta_{21}\kappa_1\kappa_2 S_1^0 S_2^0}}{2}, \tag{19}$$

where, for $p = 1, 2$,

$$\kappa_p = \frac{\varepsilon_p}{(\varepsilon_p + d_p)(\gamma_p + d_p)}.$$

Results of Lemma 1 carry forward to the local asymptotic stability or instability of (18) based on the value of $\mathcal{R}_0^{(17)}$ as defined by (19).

3.1.2 The CTMC Model When $P = 2$ and $V = 1$

In this case of one virus and two species, the CTMC takes the form

$$\mathbf{X}_t = (S_1(t), S_2(t), L_1(t), L_2(t), I_1(t), I_2(t), R_1(t), R_2(t)), \quad t \in \mathbb{R}_+ \tag{20}$$

and is characterised by the transition rates in Table 3.

3.1.3 Branching Process Approximation

Theorem 3 is specialised to the $P = 2$, $V = 1$ case by letting $Z = (L_1, L_2, I_1, I_2)$ be a MBPA of the CTMC defined in (20), with infected types ℓ_{10}, ℓ_{20}, i_{10} and i_{20}. The p.g.f. (15) takes here the form, for $\mathbf{u} = (u_1^\ell, u_2^\ell, u_1^i, u_2^i)$,

$$\mathbf{F}(\mathbf{u}) = (f_1^\ell(\mathbf{u}), f_2^\ell(\mathbf{u}), f_1^i(\mathbf{u}), f_2^i(\mathbf{u})), \tag{21}$$

where

$$f_1^{\ell}(\mathbf{u}) = \frac{\varepsilon_1 u_1^i + d_1}{\varepsilon_1 + d_1} \tag{22a}$$

$$f_2^{\ell}(\mathbf{u}) = \frac{\varepsilon_2 u_2^i + d_2}{\varepsilon_2 + d_2} \tag{22b}$$

$$f_1^{i}(\mathbf{u}) = \frac{(\beta_{11} S_1^0 u_1^{\ell} + \beta_{21} S_2^0 u_2^{\ell}) u_1^i + \gamma_1 + d_1}{\Lambda_1} \tag{22c}$$

$$f_2^{l}(\mathbf{u}) = \frac{(\beta_{12} S_1^0 u_1^{\ell} + \beta_{22} S_2^0 u_2^{\ell}) u_2^i + \gamma_2 + d_2}{\Lambda_2}, \tag{22d}$$

with

$$\Lambda_p = \sum_{q=1}^{P} \beta_{qp} S_q^0 + \gamma_p + d_p, \quad p = 1, 2.$$

Solving the equation $\mathbf{F}(z) = z$ in the present case involves finding (z_1, z_2, z_3, z_4) such that

$$z_1 = \frac{\varepsilon_1 z_3 + d_1}{\varepsilon_1 + d_1}, \; z_2 = \frac{\varepsilon_2 z_4 + d_2}{\varepsilon_2 + d_2} \tag{23a}$$

$$(\beta_{11} S_1^0 z_1 + \beta_{21} S_2^0 z_2) z_3 + \gamma_1 + d_1 = (\beta_{11} S_1^0 + \beta_{21} S_2^0 + \gamma_1 + d_1) z_3 \tag{23b}$$

$$(\beta_{12} S_1^0 z_1 + \beta_{22} S_2^0 z_2) z_4 + \gamma_2 + d_2 = (\beta_{12} S_1^0 + \beta_{22} S_2^0 + \gamma_2 + d_2) z_4. \tag{23c}$$

This is easily done numerically in applications and is known by Theorem 3 to have a unique solution in $[\mathbf{0}, \mathbf{1})$ when $\mathcal{R}_0^{(17)} > 1$.

3.2 Infectious Hematopoietic Necrosis ($P_1 \leftrightarrow P_2$)

Initially observed at fish hatcheries in Oregon and Washington in the 1950s Rucker et al. (1953), Infectious Hematopoietic Necrosis (IHN) is a viral disease that affects various species of salmonids, including Sockeye Salmon (*Oncorhynchus nerka*) and Chum Salmon (*Oncorhynchus keta*). The causative agent of IHN is the Infectious Hematopoietic Necrosis virus (IHNV), which belongs to the *Rhabdoviridae* family. This virus primarily targets the hematopoietic tissues, leading to severe anaemia and necrosis. The incubation period ranges from 5 to 45 days (Spickler 2024). Clinical signs of IHN include lethargy, darkening of skin colour, haemorrhages in various organs and eventual death. Infected fish may display reduced swimming ability and impaired feeding behaviour due to anaemia caused by red blood cell destruction (Yong et al. 2019). IHN can have a significant economic impact on fish farms that raise young rainbow trout or salmon, with mortality rates reaching 90-95% in highly susceptible fish species (Dixon et al. 2016; Spickler 2024). The virus can be transmitted hori-

zontally through direct contact or vertically from infected parents to their offspring. Waterborne transmission is also possible, particularly in crowded aquaculture settings.

Assume Chum Salmon is species 1 and Sockeye Salmon is species 2. IHN can spread within and between these two species. From (23), the fixed point is solution to

$$z_1 = \frac{\varepsilon_1 z_3 + d_1}{\varepsilon_1 + d_1},\ z_2 = \frac{\varepsilon_2 z_4 + d_2}{\varepsilon_2 + d_2} \tag{24a}$$

$$\mathcal{R}_{01} z_3^2 - \left(\mathcal{R}_{01} + \frac{\beta_{11} S_2^0}{\gamma_1 + d_1}(1 - z_4) + 1\right) z_3 + 1 = 0 \tag{24b}$$

$$\mathcal{R}_{02} z_4^2 - \left(\mathcal{R}_{02} + \frac{\beta_{22} S_1^0}{\gamma_2 + d_2}(1 - z_3) + 1\right) z_4 + 1 = 0. \tag{24c}$$

Computing exact expressions of z_3 and z_4 is not easy, but from Theorem 3, this fixed point exists. The probabilities of IHN extinction and INH outbreak are:

$$\mathbb{P}_{\text{ext}}^{\text{IHN}} = \begin{cases} \left(\frac{\varepsilon_1 z_3 + d_1}{\varepsilon_1 + d_1}\right)^{\ell_{10}} \left(\frac{\varepsilon_2 z_4 + d_2}{\varepsilon_2 + d_2}\right)^{\ell_{20}} z_3^{i_{10}} z_4^{i_{20}}, & \mathcal{R}_0^{(17)} > 1 \\ 1, & \mathcal{R}_0^{(17)} < 1, \end{cases}$$
$$\mathbb{P}_{\text{outbreak}}^{\text{IHN}} = 1 - \mathbb{P}_{\text{ext}}^{\text{IHN}} \tag{25}$$

We perform a sensitivity analysis of the probability of an outbreak of the INH virus, assessing the impact of each parameter. Note that here and throughout the computational work, we assume reproduction numbers larger than 1 unless otherwise specified.

Chum salmon has a lifespan of 3 to 6 years, during which females lay between 2,000 and 4,000 eggs National Oceanic (2023a). Similarly, sockeye salmon has a lifespan of 4 to 5 years, with females laying between 2,000 and 4,500 eggs National Oceanic (2023b). Assuming an 80% hatch rate, the birth rates for Chum (species 1) and Sockeye (species 2) in (17) are within the range of [355.55, 711.11] and [355.55, 800] per year, respectively. In a study Foott et al. (2006), the incidence of infection after release ranged from 0% to 20%. These percentages do not indicate transmission rates. However, when considering the transmission rates of (17), we compute their values using the corresponding basic reproduction number. Refer to Table 4 for parameter values ranges used in the sensitivity analysis. Moreover, with an expression of the basic reproduction number of species 1 given by $\mathcal{R}_{01}$, the transmission rates are given by

$$\beta_{11} = \frac{\mathcal{R}_{01}(\varepsilon_1 + d_1)(\gamma_1 + d_1)}{\varepsilon_1 S_1^0} \tag{26a}$$

and

Table 4 Parameter ranges and values for IHN transmission between Chum Salmon (species 1) and Sockeye Salmon (species 2)

	Meaning	Range/day	
b_1	Birth rate species 1	[1, 5]	National Oceanic (2023a)
b_2	Birth rate species 2	[1, 5]	National Oceanic (2023b)
ε_1	Incubation rate of 1	[0.02, 0.2]	Spickler (2024)
ε_2	Incubation rate of 2	[0.02, 0.2]	Spickler (2024)
γ_1	Recovery rate of 1	[0.1, 0.33]	LaPatra et al. (2000)
γ_2	Recovery rate of 2	[0.1, 0.33]	LaPatra et al. (2000)
d_1	Mortality rate of 1	$[\frac{1}{6}, \frac{1}{2}]\times \frac{1}{365}]$	
d_2	Mortality rate of 2	$[\frac{1}{5}, \frac{1}{2}]\times \frac{1}{365}]$	

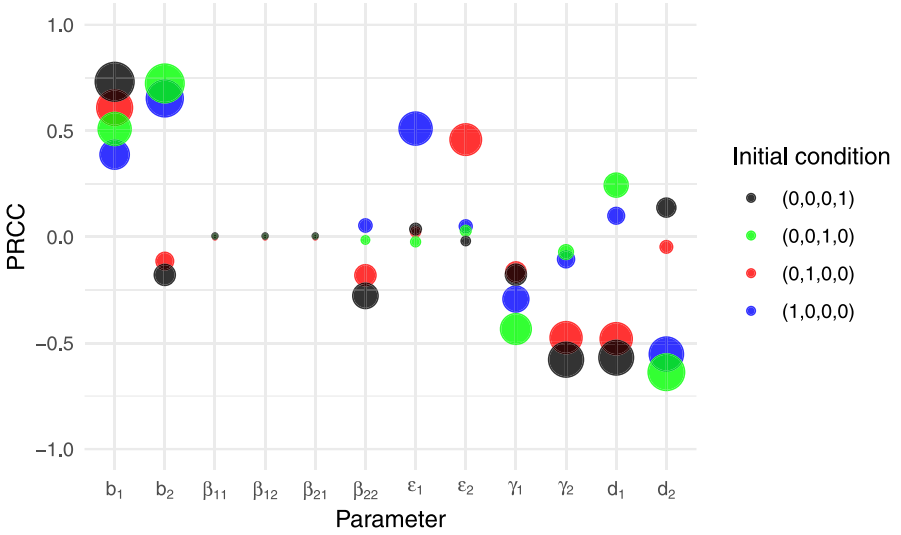

Fig. 1 Partial rank correlation coefficient (PRCC) of the probability (25) of IHN outbreak for different initial conditions $y_0 = (l_{10}, l_{20}, i_{10}, i_{20}) \in (e_1, e_2, e_3, e_4)$. The range of parameter values remaining in Table 4 (Color Figure Online)

$$\beta_{22} = \frac{\mathcal{R}_{02}(\varepsilon_2 + d_2)(\gamma_2 + d_2)}{\varepsilon_2 S_2^0}. \tag{26b}$$

We assume that the infection rate of species 2 by species 1 and species 1 by species 2 is five times higher than the infection rate within species 1 and species 2, respectively, i.e., $\beta_{21} = 5\beta_{11}$ and $\beta_{12} = 5\beta_{22}$.

Figure 1 presents a sensitivity analysis of the probability of disease outbreak, illustrating the significant impact of incubation rates on the probability of an IHN outbreak. Also important are demographic parameters b_i and d_i.

3.3 Transmission from Wild to Farmed Fish ($P_1 \to P_2, P_2 \not\to P_1$)

Interactions between wild and farmed fish populations are complex and crucial aspects of ecological and economic landscapes. In the scenario where wild fish could penetrate the space where fish are farmed, the potential transmission of diseases between these populations becomes a significant concern (Arechavala-Lopez et al. 2013). Note that contamination of wild fish by farm fish is also of concern (Johansen et al. 2011; Krkosek et al. 2007).

The situation we consider here has wild fish (species 1) able to introduce diseases to farmed populations, while farmed fish (species 2) cannot transmit diseases to wild fish, because they are raised in captivity. This asymmetry in transmission dynamics implies that (20) is considered with $\beta_{21} \neq 0$, while $\beta_{12} = 0$.

It follows that the fixed point relations (23) take the form

$$z_1 = \frac{\varepsilon_1 z_3 + d_1}{\varepsilon_1 + d_1}, \quad z_2 = \frac{\varepsilon_2 z_4 + d_2}{\varepsilon_2 + d_2}, \quad z_3 = \frac{1}{\mathcal{R}_{01}}, \tag{27a}$$

$$\mathcal{R}_{02} z_4^2 - (\mathcal{R}_{02} + c + 1)\, z_4 + 1 = 0. \tag{27b}$$

where we have denoted $c = \beta_{21}(\mathcal{R}_{01} - 1)(\gamma_1 + d_1)/(\beta_{11}(\gamma_2 + d_2))$ and

$$\mathcal{R}_{02} = \frac{\beta_{22}\varepsilon_2 S_2^0}{(\varepsilon_2 + d_1)(\gamma_2 + d_1)} \tag{28}$$

the basic reproduction for the pathogen in species 2 *in the absence of contact* with species 1.

To solve (27b), we first consider the discriminant and using the fact the $c > 0$,

$$D = (\mathcal{R}_{02} + c + 1)^2 - 4\mathcal{R}_{02} > (\mathcal{R}_{02} + 1)^2 - 4\mathcal{R}_{02} = (\mathcal{R}_{02} - 1)^2 > 0.$$

Therefore, (27b) has two real solutions z_4^- and z_4^+ given by

$$z_4^- = \frac{(\mathcal{R}_{02} + c + 1) - \sqrt{D}}{2\mathcal{R}_{02}} \quad \text{and} \quad z_4^+ = \frac{(\mathcal{R}_{02} + c + 1) + \sqrt{D}}{2\mathcal{R}_{02}}.$$

Given that $\mathcal{R}_{02} > 1$, both z_4^- and z_4^+ are positive, $z_4^+ > z_4^-$, and $z_4^+ z_4^- = 1/\mathcal{R}_{02}$. Moreover, since $D > (\mathcal{R}_{02} - 1)^2$, we obtain

$$z_4^+ > 1 + \frac{c}{2\mathcal{R}_{02}} \Longrightarrow z_4^+ z_4^- > z_4^- \Longrightarrow z_4^- < \frac{1}{\mathcal{R}_{02}}.$$

Thus, $z_4^+ > 1$, $z_4^- < 1$ and solution to the fixed point problem has

$$z_4 := z_4^- = \frac{(\mathcal{R}_{02} + c + 1) - \sqrt{(\mathcal{R}_{02} + c + 1)^2 - 4\mathcal{R}_{02}}}{2}. \tag{29}$$

Table 5 Parameter ranges and values for transmission from wild to farmed fish

Parameter	Range	Value
$\mathcal{R}_0$	[0.1, 5]	-
b_1	[2, 20]	8
b_2	[2, 20]	10
ε_1	[0.01, 0.2]	0.05
ε_2	[0.01, 0.2]	0.05
γ_1	[0.01, 0.1]	0.02
γ_2	[0.01, 0.1]	0.02
d_1	$[\frac{1}{10}, \frac{1}{2}]\times \frac{1}{365}$	-
d_2	$[\frac{1}{10}, \frac{1}{2}]\times \frac{1}{365}$	-

Then the probability of extinction of the disease in a wild-to-farmed ($W \to F$) context

$$\mathbb{P}_{\text{ext}}^{W\to F} = \begin{cases} z_1^{\ell_{10}} z_2^{\ell_{20}} z_3^{i_{10}} z_4^{i_{20}} & \mathcal{R}_{01}, \mathcal{R}_{02} > 1 \\ 1, & \mathcal{R}_{01}, \mathcal{R}_{02} \leq 1, \end{cases}$$

where z_1, z_2 and z_3 are given by (27a) and z_4 by (29); furthermore,

$$\mathbb{P}_{\text{outbreak}}^{W\to F} = 1 - \mathbb{P}_{\text{ext}}^{W\to F}. \tag{30}$$

For the sensitivity analysis of (30), we utilized the assumed parameter values provided in Table 5. The parameter ranges for β_{11} and β_{21} were computed using the relations given in (26a) and (26b).

Sensitivity analysis of disease outbreak probability $\mathbb{P}_{\text{outbreak}}^{W\to F}$ (30) (Figure 2) shows that birth (b_1), death (d_1) and recovery (γ_1) rates of species 1 are key drivers of the probability of an outbreak, regardless of initial conditions. Interestingly, for the incubation rates (ε_1 and ε_2) of species 1 and 2, respectively, there is a notable difference in impact based on the initial condition. The PRCC is 0.3 and 0.22 for the initial condition starting with one latent individual in Species 1 and Species 2, respectively, while it is very small when initially starting with infected individuals.

In contrast, factors such as infection rates β of both species and death rate of species 2 exert minimal influence on the probability of an outbreak. Moreover, specific cases involving parameters γ_2 and d_1 exhibit interesting patterns depending on where the infection starts. For instance, these parameters show a positive impact when the infection originates within species 1 but have a negative impact if it starts in species 2.

Focusing on sensitivity to mortality rates, we observe that effects can be both positive and negative. To investigate this further, we consider in Figure 3 the probability $\mathbb{P}_{\text{outbreak}}^{W\to F}$ of an outbreak as a function of the mortality rates d_1 and d_2 of species 1 and 2, respectively. When the infections start with one infectious individual in species 1, the probability of an outbreak is between 0.55 and 1. When the disease starts with one infectious individual of species 2, this range narrows to between 0.9 and 1. For initial infections in species 1, it is primarily the mortality rate of species 2 that impacts the

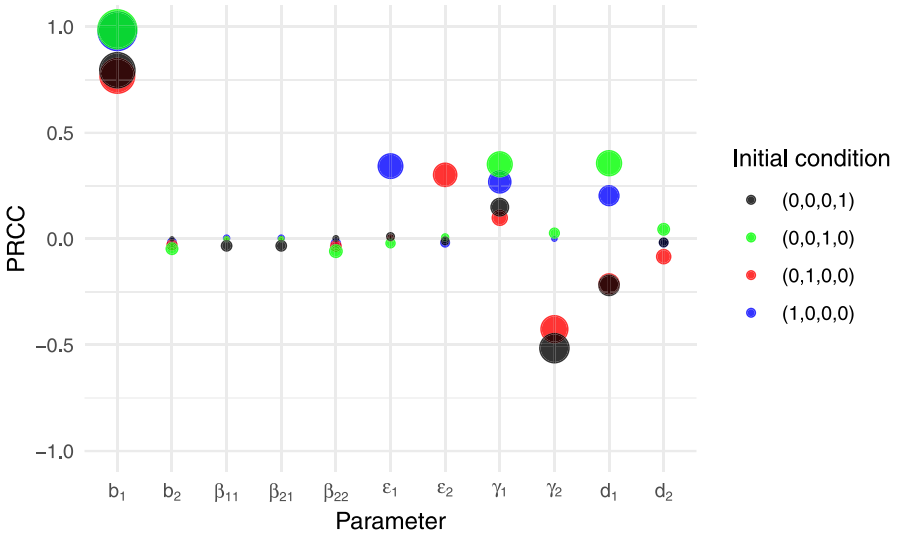

Fig. 2 PRCC of the probability (30) of disease outbreak $\mathbb{P}^{W\to F}_{\text{outbreak}}$ for four different initial conditions $y_0 = (\ell_{10}, \ell_{20}, i_{10}, i_{20}) \in (e_1, e_2, e_3, e_4)$. Parameter values ranges in Table 5 (Color Figure Online)

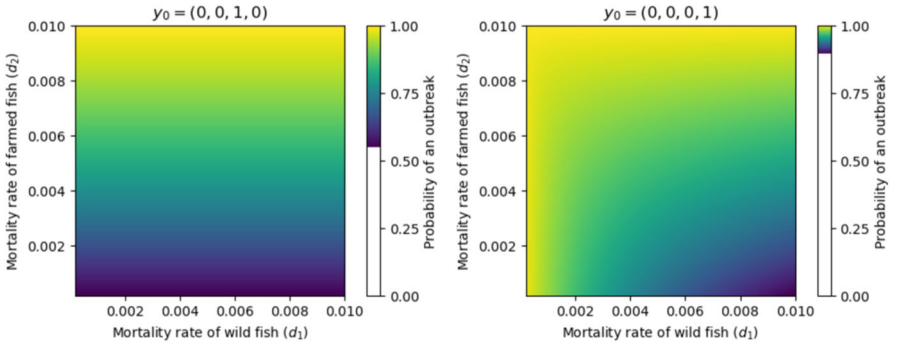

Fig. 3 Probability (30) of disease outbreak as a function of mortality rates of wild and farmed fish. For two initial conditions $y_0 = (\ell_{10}, \ell_{20}, i_{10}, i_{20}) \in (e_3, e_4)$. Parameter values in Table 4, with $\beta_{11} = \beta_{22} = 10^{-5}$, $\beta_{21} = 5\beta_{11}$ (Color Figure Online)

value of this probability. In contrast, when the infection is initiated by species 2, both mortality rates play a role in determining the outcome. Specifically, as the mortality rate d_1 of species 1 increases, there is a decrease in the probability of an outbreak, while an increase in d_2 leads to a higher probability value. Thus, initial infections in different species can lead to varying probabilities of outbreak.

3.4 Viral Hemorrhagic Septicaemia ($P_1 \to P_2, P_2 \not\to$)

Viral Hemorrhagic Septicaemia (VHS) is a highly contagious and deadly disease that affects various species of fish in both cultured and wild populations. It is prevalent

in freshwater and marine environments across several regions of the Northern Hemisphere (Gagné et al. 2007; Meyers and Winton 1995; Takano et al. 2001). VHS is caused by the Viral Hemorrhagic Septicemia Virus (VHSV) and was first isolated in Alaska from skin lesion material of two Pacific cod *Gadus macrocephalus* (Meyers et al. 1992). VHSV is known for causing hemorrhagic septicemia, which leads to severe internal bleeding and organ damage in infected fish. The symptoms vary depending on the species and the stage of infection. Some common signs include lethargy, loss of appetite, abnormal swimming behaviour and external haemorrhaging. Over 100 species of freshwater and marine fish have been reported to be naturally or experimentally susceptible to VHSV (Batts et al. 2020). These species include the Pacific herring *Clupea pallasii* Kocan et al. (2001); Meyers et al. (1994).

We consider the latter as species 1 in (17). We suppose that the latent stage is an enzootic stage, the infectious stage is the combination of disease amplification and outbreak stage and the recovery stage combines recovery and refractory as suggested by Mitro and White (2008). Now, while VHSV can infect a wide range of fish, not all infected individuals show signs of clinical disease and not all are capable of transmitting the virus to others (Ord et al. 1976). So we consider as species 2 the hybrid fry, Steelhead trout (*Salmo gairdneri*)×Coho Salmon (*Oncorhynchus kisutch*), which can get infected, but whose ability to transmit VHS has not been demonstrated (Ord et al. 1976), further simplifying the situation by making the assumption that this hybrid fry cannot transmit VHS. As a consequence, $\beta_{121} = 0$ and $\beta_{221} = 0$. Then, the fixed point relations (23) become

$$z_1 = \frac{\varepsilon_1 z_3 + d_1}{\varepsilon_1 + d_1}, \; z_2 = \frac{\varepsilon_2 z_4 + d_2}{\varepsilon_2 + d_2} \tag{31a}$$

$$\mathcal{R}_{01} z_3^2 - (\mathcal{R}_{01} + 1) z_3 + 1 = 0 \tag{31b}$$

$$\beta_{21} S_1^0 z_1 z_4 + \gamma_2 + d_2 = (\beta_{21} S_1^0 + \gamma_2 + d_2) z_4 \tag{31c}$$

where we have denoted

$$\mathcal{R}_{01} = \frac{\beta_{11}\varepsilon_{11} S_1^0}{(\varepsilon_{11} + d_1)(\gamma_{11} + d_1)} \tag{32}$$

the basic reproduction for species 1 and the virus *in the absence of contact* with species 2.

Solving (31) yields

$$(1, 1, 1, 1) \text{ and } (z_1, z_2, z_3, z_4)$$

where

$$z_1 = \frac{\varepsilon_1 z_3 + d_1}{\varepsilon_1 + d_1}, \; z_2 = \frac{\varepsilon_2 z_4 + d_2}{\varepsilon_2 + d_2}, \; z_3 = \frac{1}{\mathcal{R}_{01}}, \; z_4 = \frac{1}{c+1} \tag{33}$$

with $c = \beta_{21}(\mathcal{R}_{01} - 1)(\gamma_1 + d_1)/(\beta_{11}(\gamma_2 + d_2))$.

Therefore, the probability of extinction (no outbreak) is one if $\mathcal{R}_{01} \leq 1$, but less than one if $\mathcal{R}_{01} > 1$. Given the initial conditions $L_1(0) = \ell_{10}$, $I_1(0) = i_{10}$, $L_2(0) = \ell_{20}$, and $I_2(0) = i_{20}$, it follows from the independent branching process approximation that the probabilities of the disease extinction and the disease outbreak are

$$\mathbb{P}_{\text{ext}}^{\text{VHS}} = \begin{cases} z_1^{\ell_{10}} z_2^{\ell_{20}} z_3^{i_{10}} z_4^{i_{20}}, & \mathcal{R}_{01} > 1 \\ 1, & \mathcal{R}_{01} \leq 1, \end{cases}$$
$$\mathbb{P}_{\text{outbreak}}^{\text{VHS}} = 1 - \mathbb{P}_{\text{ext}}^{\text{VHS}}, \tag{34}$$

where the expressions of z_1, z_2, z_3 and z_4 are given in (33).

On average, a female Pacific herring lays 20,000 eggs each year (Alaska Department 2024). If we suppose that the viable percentage of the population is around 60%, then $b_1 = 12000/year \approx 33/day$. In laboratory experiments with infected herring, it was observed that shed VHSV can be identified in water within 4-5 days after exposure (PE), preceding the onset of host mortality due to the disease. The peak of viral shedding occurs between 6-10 days PE (Garver and Hawley 2021). We then consider the incubation period of 5-100 days. The duration of recovery varied depending on the phase of the epizootic. During the acute phase, which occurred around day 13 post-exposure, virus loads in tissues were significantly higher compared to the recovery phase, which spanned days 30 to 42 Hershberger et al. (2010); for sensitivity analysis of this duration is taken between 20 and 100 days. We suppose hybrid fry averaging 12,000 eggs per year with 80% viability, giving $b_2 = 9600/year = 26.3/day$. For the sensitivity analysis of the probability $\mathbb{P}_{\text{outbreak}}^{\text{VHS}}$ of VHS outbreak, the range of parameter values are given in Table 6, (26a) and (26b) is used to compute infection rates.

In Fig. 4, a sensitivity analysis of the probability of disease outbreak $\mathbb{P}_{\text{outbreak}}^{\text{VHS}}$ is presented for four different initial conditions. The birth rate b_1 of species 1 stands out as having a significant impact on the probability of an outbreak regardless of the initial condition. When the infection begins with one latent and one infectious individual in species 2, parameters b_1, γ_1, γ_2, and d_1 all exhibit a similar level of impact on the probability of an outbreak. The mortality rate d_1 of species 1 shows varying effects on the probability of an outbreak depending on where the disease originates. When the infection starts in species 2, d_1 has a significantly positive impact on the likelihood of an outbreak. However, this impact becomes negative when the disease originates in species 1.

Amongst all parameters analysed, certain factors show no discernible impact on the probability of an outbreak. This includes parameter b_2, as well as transmission rates β_{11} and β_{21}.

These findings highlight which variables have little to no effect on influencing whether a disease outbreak will occur. Moreover, the influence of different initial conditions on outcomes is a crucial aspect to consider.

3.5 The Pathogen is Endemic in One Species ($P_1^\star \to P_2$)

The problem motivating this study concerns vagrant species coming in contact with resident species while bearing a pathogen the resident species has not been exposed to yet.

To model this situation, we artificially impose that species 1 be at an endemic equilibrium while species 2 be at a disease-free equilibrium. A situation with mixed

Table 6 Parameter range and values for (17) with two species, Pacific herring (species 1) and hybrid fry (species 2) and one pathogen, VHS

	Meaning	Range	Values	Ref
$\mathcal{R}_{01}$	Basic reproduction number	[0.1, 5]		
b_1	Birth rate Pacific herring	[10, 50]	33	Alaska Department (2024)
b_2	Birth rate hybrid fry	[10, 30]	26.3	
ε_1	Incubation rate of Pacific herring	[0.01, 0.2]	0.02	Garver and Hawley (2021)
ε_2	Incubation rate of hybrid fry	[0.01, 0.2]	0.02	Garver and Hawley (2021)
γ_1	Recovery rate of Pacific herring	[0.01, 0.05]	0.03	Hershberger et al. (2010)
γ_2	Recovery rate of hybrid fry	[0.01, 0.05]	0.03	Hershberger et al. (2010)
d_1	Mortality rate of species 1	$[\frac{1}{15}, \frac{1}{2}]\times \frac{1}{365}$	3.10^{-4}	Alaska Department (2024); Stokesbury et al. (2002)
d_2	Mortality rate of species 2	$[\frac{1}{15}, \frac{1}{2}]\times \frac{1}{365}$	3.10^{-4}	

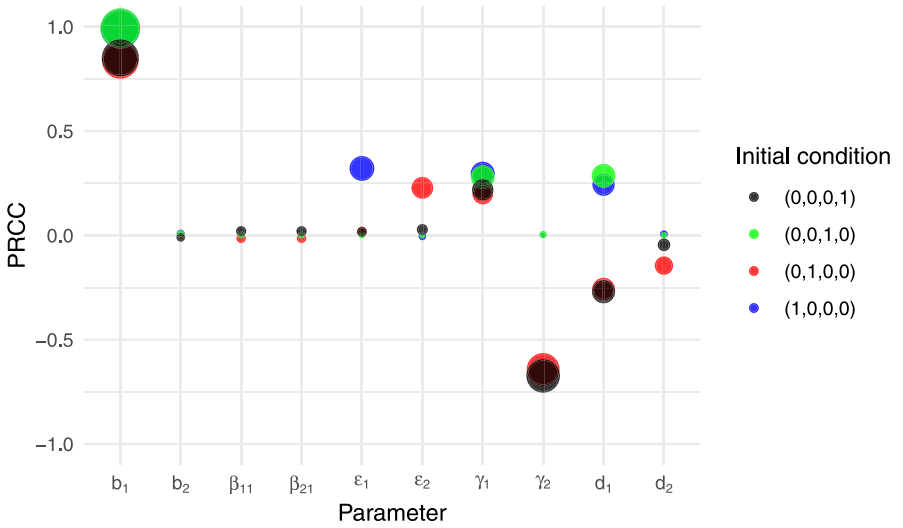

Fig. 4 PRCC of the probability of disease outbreak (34) for different initial conditions $y_0 = (\ell_{10}, \ell_{20}, i_{10}, i_{20}) \in (e_1, e_2, e_3, e_4)$. Parameter values ranges in Table 6

equilibria of this type is not possible in (17), so we "cheat": we start by assuming that both species are not in contact and that species 1 is at the endemic equilibrium $E_1^\star := (S_1^\star, L_1^\star, I_1^\star, R_1^\star)$, in which

$$E_1^\star = \left(\frac{S_1^0}{\mathcal{R}_{01}}, \frac{(\mathcal{R}_{01}-1)(\gamma_1+d_1)d_1}{\beta_{11}\varepsilon_1}, \frac{(\mathcal{R}_{01}-1)d_1}{\beta_{11}}, \frac{(\mathcal{R}_{01}-1)\gamma_1}{\beta_{11}} \right), \tag{35}$$

where $\mathcal{R}_{01}$ given by (32) is the basic reproduction for the pathogen in species 1 in the absence of contact with species 2. We suppose that this determines the dynamics of the pathogen in species 1, which we now ignore except insofar as the infecting potential of the $I_1^\star$ individuals from species 1 infectious with the pathogen potentially coming into contact with susceptible individuals from species 2. We then consider the second population, focusing on conditions leading to the disease becoming established there.

3.5.1 The ODE Introduction Model

Given a prevalence of infection $I_1^\star$ in species 1, the infection dynamics in species 2 is governed by

$$\dot{S}_2 = b_2 - \beta_{21} I_1^\star S_2 - \beta_{22} S_2 I_2 - d_2 S_2 \tag{36a}$$
$$\dot{L}_2 = \beta_{21} I_1^\star S_2 + \beta_{22} S_2 I_2 - (\varepsilon_2 + d_2) L_2 \tag{36b}$$
$$\dot{I}_2 = \varepsilon_2 L_2 - (\gamma_2 + d_2) I_2 \tag{36c}$$
$$\dot{R}_2 = \gamma_2 I_2 - d_2 R_2, \tag{36d}$$

considered with nonnegative initial conditions.

Model (36) is not a classic immigration model, since the term $\beta_{21} I_1^\star$ is factor of S_2, not a constant. However, similarly to immigration models, the term $\beta_{21} I_1^\star S_2$ in (36b) precludes the existence of a disease-free equilibrium for (36). As a consequence, no basic reproduction number can be computed for (36). The method of Almarashi and McCluskey (2019) is not applicable here since immigration occurs at the *per capita* rate $\beta_{21} I_1^\star$, not at a constant rate. The term $\beta_{21} I_1^\star$ cannot be considered as encoding horizontal transmission either, at least not in the usual sense, since inflow into (36b) is function of S_2, not I_2.

As a consequence, a thorough analysis of properties of (36) is difficult and beyond the scope of this work. Instead, we focus on simple properties as well as computational considerations.

System (36) admits a unique equilibrium, an endemic equilibrium taking the form $E_2^\star := (S_2^\star, L_2^\star, I_2^\star, R_2^\star)$, where

$$S_2^\star = \frac{\varepsilon_2 + d_2}{\beta_{21} I_1^\star + \beta_{22} I_2^\star} L_2^\star, \quad L_2^\star = \frac{\gamma_2 + d_2}{\varepsilon_2} I_2^\star, \quad R_2^\star = \frac{\gamma_2 I_2^\star}{d_2}$$

and $I_2^\star$ is a root of the second order polynomial

$$\beta_{22} (I_2^\star)^2 - ((\mathcal{R}_{02} - 1) d_2 - \beta_{21} I_1^\star) I_2^\star - \frac{\beta_{21} d_2 I_1^\star \mathcal{R}_{02}}{\beta_{22}} = 0, \tag{37}$$

where $\mathcal{R}_{02}$ given in (28) is the basic reproduction for species 2 and the virus *in the absence of contact* with species 1.

Since the coefficients $\beta_{22} > 0$ and $\beta_{21} \mathcal{R}_{02} I_1^\star / \beta_{22} > 0$, Descartes rule of signs implies that the polynomial (37) has a unique positive solution. The expression of this solution is given by

$$I_2^\star = \frac{(\mathcal{R}_{02} - 1) d_2 - \beta_{21} I_1^\star + \sqrt{((\mathcal{R}_{02} - 1) d_2 - \beta_{21} I_1^\star)^2 + 4 \mathcal{R}_{02} d_2 \beta_{21} I_1^\star}}{2 \beta_{22}}. \tag{38}$$

In Fig. 5, we show how (equilibrium) prevalence of infection in species 2 depends on prevalence of infection in species 1. For low values of the reproduction number in species 2, the situation is quite dependent on the prevalence of infection in the "introducing species", but as the reproduction number increases, this dependence diminishes to the point of the situation becoming indistinguishable for large values of $\mathcal{R}_{02}$.

3.5.2 The CTMC Introduction Model

Note that it is not possible here to use a multitype branching process approximation, for roughly the same reasons that a basic reproduction number does not exist for the deterministic model (36). Indeed, while branching processes incorporating *immigration* exist (Heathcote 1965; Pakes 1971), they assume that immigration is a process

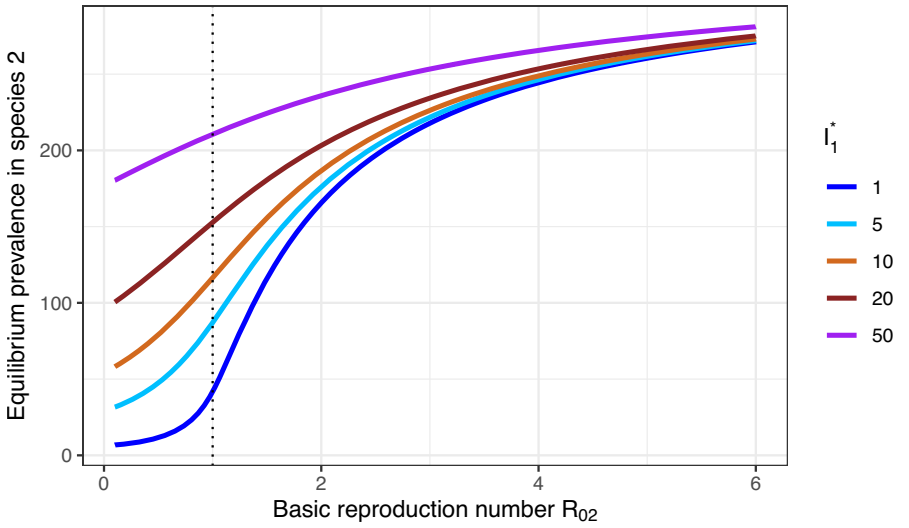

Fig. 5 Equilibrium prevalence of infection $I_2^\star$ in population 2 as a function of the reproduction number $\mathcal{R}_{02}$ for the pathogen in species 2. The different curves correspond to different values of prevalence $I_1^\star$ in population 1 (Color Figure Online)

that is independent from the population immigrants are joining. In our model, this is not true, since "immigration" depends on the susceptible population S_2. So we focus here on the computational analysis of the CTMC. In all results presented here, 10,000 simulations (realisations) of the CTMC associated to (36) are used for each data point.

Figure 6 shows the percentage of 10K simulations in which at least one transmission occurs from species 1 to species 2 (red curve) and from species 2 to species 2 (green curve). Simulations assume that $\mathcal{R}_{02} = 1.5$ and are run for 90 days. Note that the latter type of transmission always requires that introduction by species 1 has taken place. Additionally, we show the percentage of realisations in which spread by species 1 occurs followed by extinctions, where we characterise an extinction of the infection in species 2 as a moment when the total number of infected in species 2, $L_2(t) + I_2(t)$, is zero after having been positive.

This illustrates a very important part of the introduction process. In keeping with the terminology in Arino et al. (2021, 2020), let us assess success of an introduction from the perspective of the pathogen. In view of Fig. 6, what drives successful introductions is the size of the introduction, i.e., the so-called *inoculum size*. However, before it becomes established in species 2 (the consequence of which is shown in a deterministic context by Fig. 5), the infection in species 2 must "survive" the *stochastic phase* of the epidemic; see, e.g., the one location case in Arino and Milliken (2022). This illustrates that spillover events are often unsuccessful, as observed in the zoonotic case with bats Sánchez et al. (2022).

To better understand this issue, consider Fig. 7, where we show violin plots of the distribution of times at which the first infection in species 2 arises stemming from contact with, respectively, species 1 and species 2. These values are from the same simulations as used in Fig. 6 and thus represent the percentages shown there of 10K

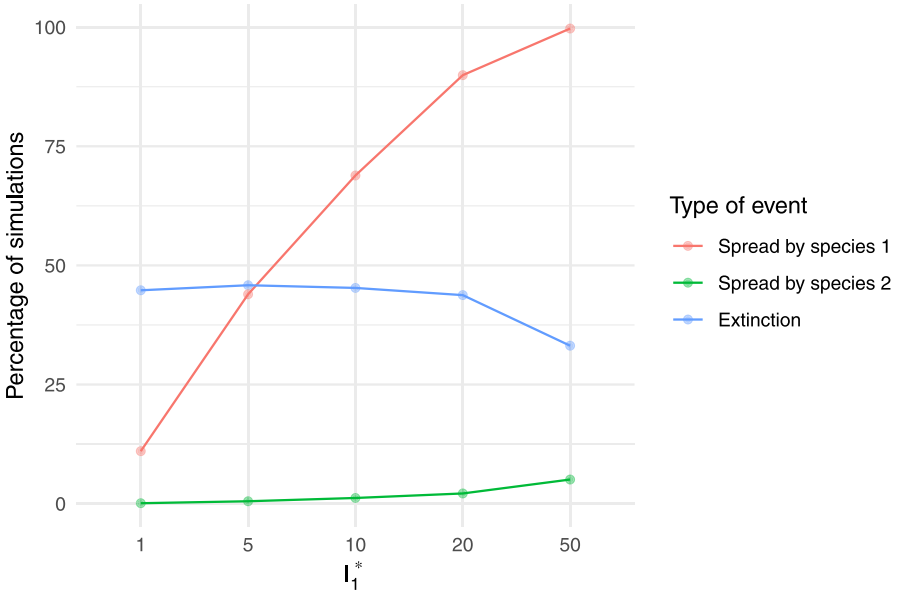

Fig. 6 Percentage of 10K realisations in which spread by species 1 (introductions) and species 2 occurs. Also shown is the percentage of realisations where introductions by species 1 are followed by extinctions

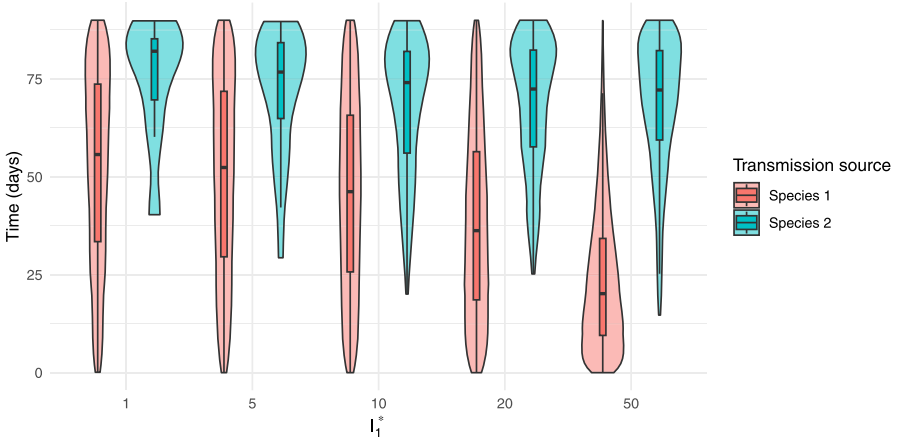

Fig. 7 Distribution of the times at which the first infection event occurs in species 2 following contact with an infected individual from species 1 (red) and species 2 (blue), for different values of $I_1^\star$. Boxplots within the violins show the median, interquartile range and whiskers extents

simulations. First, consider infections with source species 1, i.e., introductions into species 2. We observe that as the prevalence $I_1^\star$ in species 1 increases, the time to first introduction progressively diminishes, with the interquartile range covering smaller and smaller values. Now consider the timing of infections originating from species 2, i.e., taking place after the infection has become somewhat established in species 2. There, we observe that as the prevalence $I_1^\star$ increases, times to the first transmission

decrease, but not as acutely as those to the first introduction. This confirms our earlier observation that introduction and establishment, although evidently correlated, are not as tightly tied as can be expected.

4 Case of Two Pathogens and Two Species

Here the dynamics with $P = 2$ species and $V = 2$ pathogens are considered. While the cases in Sect. 3 are more tractable mathematically, the situation here is more realistic. In practice, the collaboration motivating this work is interested in over a dozen pathogens potentially infecting four fish species. We do not consider such a general situation here, but illustrate the computational complexities that arise even when $P = V = 2$. One particularly interesting feature is the existence of mixed equilibria, i.e., equilibria in which one of the pathogens is present and the other absent.

4.1 Deterministic Model and Basic Analysis

$$\dot{S}_1 = b_1 - \left(\sum_{q=1}^{2}\sum_{v=1}^{2}\beta_{1qv}I_{qv} + d_1\right)S_1, \qquad \dot{S}_2 = b_2 - \left(\sum_{q=1}^{2}\sum_{v=1}^{2}\beta_{2qv}I_{qv} + d_2\right)S_2, \tag{39a}$$

$$\dot{L}_{11} = \sum_{q=1}^{2}\beta_{1q1}I_{q1}S_1 - (\varepsilon_{11} + d_1)L_{11}, \qquad \dot{L}_{21} = \sum_{q=1}^{2}\beta_{2q1}I_{q1}S_2 - (\varepsilon_{21} + d_2)L_{21}, \tag{39b}$$

$$\dot{L}_{12} = \sum_{q=1}^{2}\beta_{1q2}I_{q2}S_1 - (\varepsilon_{12} + d_1)L_{12}, \qquad \dot{L}_{22} = \sum_{q=1}^{2}\beta_{2q2}I_{q2}S_2 - (\varepsilon_{22} + d_2)L_{22}, \tag{39c}$$

$$\dot{I}_{11} = \varepsilon_{11}L_{11} - (\gamma_{11} + d_1)I_{11}, \qquad \dot{I}_{21} = \varepsilon_{21}L_{21} - (\gamma_{21} + d_2)I_{21}, \tag{39d}$$

$$\dot{I}_{12} = \varepsilon_{12}L_{12} - (\gamma_{12} + d_1)I_{12}, \qquad \dot{I}_{22} = \varepsilon_{22}L_{22} - (\gamma_{22} + d_2)I_{22}, \tag{39e}$$

$$\dot{R}_1 = \sum_{v=1}^{2}\gamma_{1v}I_{1v} - d_1R_1, \qquad \dot{R}_2 = \sum_{v=1}^{2}\gamma_{2v}I_{2v} - d_2R_2. \tag{39f}$$

The disease-free equilibrium of (39) is

$$\boldsymbol{E}_0^{(39)} = (S_1^0, S_2^0, 0_{\mathbb{R}^{10}}), \quad \text{with } S_1^0 = \frac{b_1}{d_1} \text{ and } S_2^0 = \frac{b_2}{d_2}. \tag{40}$$

To compute the basic reproduction number $\mathcal{R}_0$, observe that the matrices $\mathbf{G}_{12}$ and $\mathbf{W}$ derived in Sect. 2.3 take here the form

$$\mathbf{G}_{12} = \begin{bmatrix} \mathbf{G}_{12}^{11} & \mathbf{G}_{12}^{12} \\ \mathbf{G}_{12}^{21} & \mathbf{G}_{12}^{22} \end{bmatrix},$$

where $\mathbf{G}_{12}^{11} = S_1^0 \mathsf{diag}(\beta_{111}, \beta_{112}), \mathbf{G}_{12}^{12} = S_1^0 \mathsf{diag}(\beta_{121}, \beta_{122}), \mathbf{G}_{12}^{21} = S_2^0 \mathsf{diag}(\beta_{211}, \beta_{212})$ and $\mathbf{G}_{12}^{22} = S_2^0 \mathsf{diag}(\beta_{221}, \beta_{222})$ are diagonal matrices, and S_1^0 and S_2^0 are scalars. The matrix $\mathbf{W}$ is block lower triangular, with blocks

$$\begin{aligned} \mathbf{W_{11}} &= \mathsf{diag}(d_1 + \varepsilon_{11}, d_1 + \varepsilon_{12}, d_2 + \varepsilon_{21}, d_2 + \varepsilon_{22}), \\ \mathbf{W_{21}} &= \mathsf{diag}(\varepsilon_{11}, \varepsilon_{12}, \varepsilon_{21}, \varepsilon_{22}) \end{aligned}$$

and

$$\mathbf{W_{22}} = \mathsf{diag}(d_1 + \gamma_{11}, d_1 + \gamma_{12}, d_2 + \gamma_{21}, d_2 + \gamma_{22}).$$

The basic reproduction number of system (39) following the formula in equation (8) is given by:

$$\mathcal{R}_0^{(39)} = \max(\mathcal{R}_0^1, \mathcal{R}_0^2)$$

where $\mathcal{R}_0^1 = \rho(\mathcal{B}_1)$ and $\mathcal{R}_0^2 = \rho(\mathcal{B}_2)$, with the matrices $\mathcal{B}_1$ and $\mathcal{B}_2$ obtained by using a form of a matrix in equation (9), and then

$$\mathcal{B}_1 = \begin{pmatrix} \frac{\beta_{111}\varepsilon_{11}S_1^0}{(\varepsilon_{11}+d_1)(\gamma_{11}+d_1)} & \frac{\beta_{121}\varepsilon_{21}S_1^0}{(\varepsilon_{21}+d_2)(\gamma_{21}+d_2)} \\ \frac{\beta_{211}\varepsilon_{11}S_2^0}{(\varepsilon_{11}+d_1)(\gamma_{11}+d_1)} & \frac{\beta_{221}\varepsilon_{21}S_2^0}{(\varepsilon_{21}+d_2)(\gamma_{21}+d_2)} \end{pmatrix}, \mathcal{B}_2 = \begin{pmatrix} \frac{\beta_{112}\varepsilon_{12}S_1^0}{(\varepsilon_{12}+d_1)(\gamma_{12}+d_1)} & \frac{\beta_{122}\varepsilon_{22}S_1^0}{(\varepsilon_{22}+d_2)(\gamma_{22}+d_2)} \\ \frac{\beta_{212}\varepsilon_{12}S_2^0}{(\varepsilon_{12}+d_1)(\gamma_{12}+d_1)} & \frac{\beta_{222}\varepsilon_{22}S_2^0}{(\varepsilon_{22}+d_2)(\gamma_{22}+d_2)} \end{pmatrix} \tag{41}$$

Note that the result provided by using $\mathcal{R}_0^{(39)}$ does not show the whole picture. Indeed, one interesting characteristic of (1) is that the viruses function in a disconnected way. This can be inferred from the reducibility of the system discussed in Appendix A.

Theorem 4 *Consider (39) with $\mathcal{R}_{01} > 1$ and $\mathcal{R}_{02} \leq 1$. Then the DFE of (39) is unstable and consists of a mixed equilibrium wherein pathogen 1 is present at an endemic level and pathogen 2 is absent. Stability of the pathogen-2-free equilibrium is global and asymptotic with respect to the pathogen-2 subsystem.*

The existence part of the proof of this result is shown in Appendix D. Global asymptotic stability of the pathogen-2-free equilibrium follows directly from Theorem 2 and reducibility of the system.

4.2 Branching Process Approximation

Let $Z = (L_{11}, L_{12}, L_{21}, L_{22}, I_{11}, I_{12}, I_{21}, I_{22})$ be the multitype branching process approximation of CTMC $X^{2,2}(t)$ with infected types $\ell_{11}, \ell_{12}, \ell_{21}, \ell_{22}, i_{11}, i_{12}, i_{21}$ and

i_{22}. The p.g.f. for $\mathbf{u} = (u_{11}^{\ell}, u_{12}^{\ell}, u_{21}^{\ell}, u_{22}^{\ell}, u_{11}^{i}, u_{21}^{i}, u_{21}^{i}, u_{22}^{i})$ is defined as

$$\mathbf{F}(\mathbf{u}) = (f_{11}^{\ell}(\mathbf{u}), f_{12}^{\ell}(\mathbf{u}), f_{21}^{\ell}(\mathbf{u}), f_{22}^{\ell}(\mathbf{u}), f_{11}^{i}(\mathbf{u}), f_{21}^{i}(\mathbf{u}), f_{21}^{i}(\mathbf{u}), f_{22}^{i}(\mathbf{u})), \tag{42}$$

where, for $p, v = 1, 2$,

$$f_{pv}^{\ell}(\mathbf{u}) = \frac{\varepsilon_{pv} u_{pv}^{i} + d_p}{\varepsilon_{pv} + d_p}, \tag{43a}$$

$$f_{pv}^{i}(\mathbf{u}) = \frac{\left(\sum_{q=1}^{2} \beta_{qpv} S_q^0 u_{pv}^{\ell}\right) u_{pv}^{i} + \gamma_{pv} + d_p}{\Lambda_{pv}}. \tag{43b}$$

The Jacobian matrix then takes the form

$$DF(u) = \begin{bmatrix} 0 & | & \mathbb{M}_{12} \\ -- & -- & -- \\ \mathbb{M}_{21} & | & \mathbb{M}_{22} \end{bmatrix},$$

where

$$\mathbb{M}_{12} = \mathsf{diag}\left(\frac{\varepsilon_{11}}{\varepsilon_{11}+d_1}, \frac{\varepsilon_{12}}{\varepsilon_{12}+d_1}, \frac{\varepsilon_{21}}{\varepsilon_{21}+d_2}, \frac{\varepsilon_{22}}{\varepsilon_{22}+d_2}\right),$$

$$\mathbb{M}_{21} = \begin{pmatrix} \frac{\beta_{111} S_1^0 u_{11}^i}{\Lambda_{11}} & 0 & \frac{\beta_{121} S_2^0 u_{11}^i}{\Lambda_{11}} & 0 \\ 0 & \frac{\beta_{112} S_1^0 u_{12}^i}{\Lambda_{12}} & 0 & \frac{\beta_{122} S_2^0 u_{12}^i}{\Lambda_{12}} \\ \frac{\beta_{211} S_1^0 u_{21}^i}{\Lambda_{21}} & 0 & \frac{S_2^0 \beta_{221} u_{21}^i}{\Lambda_{21}} & 0 \\ 0 & \frac{\beta_{212} S_1^0 u_{22}^i}{\Lambda_{22}} & 0 & \frac{\beta_{222} S_2^0 u_{22}^i}{\Lambda_{22}} \end{pmatrix}$$

and

$$\mathbb{M}_{22} = \mathsf{diag}\Bigg(\frac{\beta_{111} S_1^0 u_{11}^{\ell} + \beta_{121} S_2^0 u_{21}^{\ell}}{\Lambda_{11}}, \frac{\beta_{112} S_1^0 u_{12}^{\ell} + \beta_{122} S_2^0 u_{22}^{\ell}}{\Lambda_{12}}, \frac{\beta_{211} S_1^0 u_{11}^{\ell} + \beta_{221} S_2^0 u_{21}^{\ell}}{\Lambda_{21}}, \frac{\beta_{212} S_1^0 u_{12}^{\ell} + \beta_{222} S_2^0 u_{22}^{\ell}}{\Lambda_{22}}\Bigg).$$

Theorem 3 applies here. Given $L_{11}(0) = \ell_{110}$, $L_{12}(0) = \ell_{120}$, $L_{21}(0) = \ell_{210}$, $L_{22}(0) = \ell_{220}$, $I_{11}(0) = i_{110}$, $I_{12}(0) = i_{120}$, $I_{21}(0) = i_{210}$ and $I_{22}(0) = i_{220}$, it follows from the independent branching process approximation that the probabilities of extinction and disease outbreak are:

$$\mathbb{P}_{\text{ext}}^{(42)} = \begin{cases} (z_{11}^{\ell})^{\ell_{110}} (z_{12}^{\ell})^{\ell_{120}} (z_{21}^{\ell})^{\ell_{210}} (z_{22}^{\ell})^{\ell_{220}} (z_{11}^{i})^{i_{110}} (z_{12}^{i})^{i_{120}} (z_{21}^{i})^{i_{210}} (z_{22}^{i})^{i_{220}}, & \mathcal{R}_0^{(39)} > 1 \\ 1, & \mathcal{R}_0^{(39)} < 1, \end{cases}$$

$$\mathbb{P}_{\text{outbreak}}^{(42)} = 1 - \mathbb{P}_{\text{ext}}^{(42)} \tag{44}$$

5 Discussion

We formulated an SLIR model for the spread of V pathogens between and within P species. The model was first formulated as a set of $2P(1+V)$ ordinary differential equations, of which we considered elementary properties: basic reproduction number $\mathcal{R}_0$ and local asymptotic stability as a function of the value of the reproduction number. Global asymptotic stability when $\mathcal{R}_0 < 1$ was also established. We then considered the corresponding continuous-time Markov chain (CTMC) model, which provides a better tool to study the behaviour of the system close to the disease-free equilibrium (DFE), which is our main interest here. To do so, we employed a multitype branching process approximation of the CTMC near the DFE, obtaining an expression for the probability of an outbreak when $\mathcal{R}_0 > 1$. This probability was interpreted, in the context of our model, as the probability that the pathogen becomes established in the population, at least temporarily. (The result is local and does not address the proper establishment at an endemic level.)

The case of a single pathogen spreading between two species was then investigated computationally. A metapopulation (spatial) version of this situation with a slightly different underlying SLIR model was investigated both mathematically and computationally in Arino et al. (2005), with, using the notation here, P species present. However, focusing on just two species as we did here allows to get a better understanding of the processes. To this effect, in particular, we investigated the sensitivity of the system to its parameters in the case of three viruses affecting fish leading to very different transmission scenarios. These highlighted in particular the important role played by demographic parameters. A fourth, more abstract case concerned introduction of a pathogen in a population by another in which the pathogen is present at an endemic level.

One interesting feature of the model is that despite its complication, pathogens function more or less independently from one another. This was shown in the case $P = V = 2$, which we considered next. We conjecture that the following natural extension of Theorem 4 holds.

Conjecture 5 *Consider (1) in which pathogens* $a = 1, \ldots, k$ *have* $\mathcal{R}_{0a} < 1$ *and pathogens* $e = k+1, \ldots, V$ *have* $\mathcal{R}_{0e} > 1$*, for some* $k \in \{1, \ldots, n\}$*. Then (1) has an unstable mixed equilibrium in which pathogens* $1, \ldots, k$ *are absent and pathogens* $k+1, \ldots, V$ *are present at an endemic level.*

By Theorem 2, those pathogens that are absent would naturally be globally asymptotically stably so. This highlights a limitation of the model: because we assume that species dynamics is independent of the pathogens and that coinfections cannot occur, a situation as described by Theorem 4 or Conjecture 5 is possible. While not necessarily unrealistic, taking into account more advanced interactions between pathogens, or effects of pathogens onto their host species, could be interesting and lead to wholly different results. Competition effects between species could also be incorporated and would also likely lead to different results.

Another interesting variation could involve considering an *epidemic* model. In its current form, the model is an *endemic* model, with the basic reproduction numbers distinguishing between a situation where the disease is absent and one where the

disease is present at an endemic level. In this case, of course, the pathogen always becomes extinct; it is not clear, though, if a situation similar to that in Theorem 4 and Conjecture 5, in this case with some pathogens undergoing an epidemic and others not, would hold.

Finally, note that we considered an SLIR model, not an SLIRS model, i.e., we assumed that acquired immunity is permanent. With respect to the work carried out here, this makes very little difference. Indeed, adding a flow from R to S does not modify the expression of the disease-free equilibrium nor of the basic reproduction number, which is the focus of most of our work. The only difference between the two model formulations would appear, in the present work in the particular case where the pathogen is endemic in one species (Sect. 3.5). There, (35) would be slightly modified, but this has no consequence since $E_1^\star$ is used as a parameter. The expressions in Sect. 3.5.1 would also change, as some would incorporate the rate of movement from R to S, but the overall conclusions remain.

A Normal forms of matrices

When considering the global asymptotic stability of the DFE in Appendix B or existence of threshold behaviour in Appendix C, we observe that the matrices involved are reducible. While the presentation used in the body of the paper is the most natural, the proofs in these appendices require to use the normal form of the matrices involved. Further understanding of the reproduction number is also gained by using the normal form. Let us illustrate this using matrix A_{22} in Appendix B. The permutation matrix obtained in the process is the same for all four matrices we consider here.

It is clear that matrix A_{22} as given by (48) is reducible. Indeed, consider the weighted loop-directed graph having A_{22} as its adjacency matrix. Diagonal entries of the two main diagonal blocks correspond to loops. The blocks $\mathbf{\Psi}(\mathbf{x}_S, \mathbf{x}_I)$ and $\mathsf{diag}(\llbracket \varepsilon_{pv} \rrbracket)$, on the other hand, show that vertices form PV strongly connected components, with each component comprising 2 vertices. Consider for instance the $(1, 1)$ entry in $\mathbf{\Psi}$ and the $(1, 1)$ entry in $\mathsf{diag}(\llbracket \varepsilon_{pv} \rrbracket)$. They establish that vertex 1 is connected to vertex $PV + 1$ and that vertex $PV + 1$ is connected to vertex 1. All entries in these matrices define similar pairs of vertices, giving the PV strong components. Ordering vertices (and corresponding matrix entries) so that vertices in a strong connected component are listed consecutively, it is then easy to find the permutation matrix $\mathbf{\Pi}$ such that

$$\mathbf{\Pi}\ A_{22}(\mathbf{x}_S, \mathbf{x}_I)\mathbf{\Pi}^T = \bigoplus_{\llbracket pv \rrbracket} \begin{pmatrix} -(\varepsilon_{pv} + d_p) & \sum_{q=1}^{P} \beta_{qpv} S_q \\ \varepsilon_{pv} & -(\gamma_{pv} + d_p) \end{pmatrix}. \tag{45}$$

Applying $\mathbf{\Pi}$ to $D\mathbf{F}$ given by (50) in Appendix C, we find

$$\mathbf{\Pi}\ D\mathbf{F}(\mathbf{u}^\ell, \mathbf{u}^i)\ \mathbf{\Pi}^T = \bigoplus_{\llbracket pv \rrbracket} \begin{pmatrix} 0 & \dfrac{\varepsilon_{pv}}{\varepsilon_{pv} + d_p} \\ S_p^0 \dfrac{\beta_{pqv} u^i_{pv}}{\Lambda_{pv}} & \dfrac{\sum_{q=1}^{P} S_q^0 u^\ell_{qv}}{\Lambda_{pv}} \end{pmatrix}. \tag{46}$$

B Proof of Theorem 2

To prove global asymptotic stability of the disease-free equilibrium of (1) when $\mathcal{R}_0 < 1$, we use a result of (Kamgang and Sallet (2008),Theorems 4.3 and 4.5). For the convenience of the reader, we recall this result but with notation adapted to the problem under consideration here.

Let $\mathbf{x}_S = (\llbracket S_p \rrbracket, \llbracket R_p \rrbracket)^T \in \mathbb{R}^{2P}$ and $\mathbf{x}_I = (\llbracket L_{pv} \rrbracket, \llbracket I_{pv} \rrbracket)^T \in \mathbb{R}^{2PV}$ be, respectively, the vectors of non-infected compartments and infected compartments. Denote $\mathbf{x}_S^0 = (\llbracket S_p^0 \rrbracket, \llbracket 0 \rrbracket)^T \in \mathbb{R}^{2P}$ the part of the disease-free equilibrium of (1) corresponding to $\mathbf{x}_S$, i.e., the DFE is $(\mathbf{x}_S^0, \mathbf{0}_{2PV})$. Rewrite (1) in the following compact form,

$$\begin{aligned} \dot{\mathbf{x}}_S &= A_{11}(\mathbf{x}_S, \mathbf{x}_I)(\mathbf{x}_S - \mathbf{x}_S^0) + A_{12}(\mathbf{x}_S, \mathbf{x}_I)\mathbf{x}_I, \\ \dot{\mathbf{x}}_I &= A_{22}(\mathbf{x}_S, \mathbf{x}_I)\mathbf{x}_I, \end{aligned} \tag{47}$$

with

$$\begin{aligned} A_{11}(\mathbf{x}_S, \mathbf{x}_I) &= \begin{pmatrix} -\mathrm{diag}\left(\llbracket d_p \rrbracket\right) & \mathbf{0} \\ \mathbf{0} & -\mathrm{diag}\left(\llbracket d_p \rrbracket\right) \end{pmatrix} \in \mathbb{R}^{2P\times 2P}, \\ A_{12}(\mathbf{x}_S, \mathbf{x}_I) &= \begin{pmatrix} \mathbf{0} & -\boldsymbol{\Phi}(\mathbf{x}_S, \mathbf{x}_I) \\ \mathbf{0} & \boldsymbol{\Gamma}(\mathbf{x}_S, \mathbf{x}_I) \end{pmatrix} \in \mathbb{R}^{2P\times 2PV}, \\ A_{22}(\mathbf{x}_S, \mathbf{x}_I) &= \begin{pmatrix} -\mathrm{diag}\left(\llbracket \varepsilon_{pv} + d_p \rrbracket\right) & \boldsymbol{\Psi}(\mathbf{x}_S, \mathbf{x}_I) \\ \mathrm{diag}\left(\llbracket \varepsilon_{pv} \rrbracket\right) & -\mathrm{diag}\left(\llbracket \gamma_{pv} + d_p \rrbracket\right) \end{pmatrix} \in \mathbb{R}^{2PV\times 2PV}, \end{aligned} \tag{48}$$

where $\Phi(\mathbf{x}_S, \mathbf{x}_I)$ is a $P \times PV$-matrix whose jth row is a PV-vector with entries $\llbracket S_j \beta_{jpv} \rrbracket$, $\boldsymbol{\Gamma}(\mathbf{x}_S, \mathbf{x}_I)$ is a $P \times PV$-matrix with jth row having V nonzero entries $\gamma_{j1}, \ldots, \gamma_{jV}$ in columns $(j-1)V + 1$ to jV and $\boldsymbol{\Psi}(\mathbf{x}_S, \mathbf{x}_I)$ is a diagonal $PV \times PV$-matrix,

$$\boldsymbol{\Psi}(\mathbf{x}_S, \mathbf{x}_I) = \mathrm{diag}\left(\llbracket \sum_{q=1}^{P} \beta_{qpv} S_q \rrbracket\right),$$

with the enumerator running over indices $p = 1, \ldots, P$ and $v = 1, \ldots, V$.

As discussed in Appendix A, it is clear that matrix A_{22} as given by (48) is reducible. So we apply the method described in that Appendix and instead work with the similar normal form matrix (45). We can apply (Kamgang and Sallet (2008),Theorem 4.3) to each of the PV blocks in (45) or apply (Kamgang and Sallet (2008),Theorem 4.5), which considers the reducible case. We use a combination of the two results.

Let $\Omega \subset \mathbb{R}_+^{2P} \times \mathbb{R}_+^{2PV}$ be the set defined in the statement of Theorem 2. If the following five conditions hold true, then (Kamgang and Sallet (2008),Theorem 4.5) establishes that the disease-free equilibrium $(\mathbf{x}_S^0, \mathbf{0}_{2PV})$ is globally asymptotically stable when $\mathcal{R}_0 < 1$.

C1 System (47) is defined on a positively invariant set Ω of the nonnegative orthant and dissipative on Ω.

C2 Subsystem $\dot{\mathbf{x}}_S = A_{11}(\mathbf{x}_S, \mathbf{0})(\mathbf{x}_S - \mathbf{x}_S^0)$ is globally asymptotically stable at the disease-free equilibrium $\mathbf{x}_S^0$ on the canonical projection of Ω on $\mathbb{R}_+^{2P}$.

C3 Matrix $\tilde{A}_{22}(\mathbf{x}_S, \mathbf{x}_I)$ given by (45) is block upper triangular, with each diagonal block $\hat{A}_{22}^{pv}$ being Metzler and irreducible for any $\mathbf{x} = (\mathbf{x}_S, \mathbf{x}_I) \in \Omega$.

C4 For each p, v, there exists an upper-bound matrix $\hat{A}_{22}^{pv}$ for $M = \{A_{22}^{pv}(\mathbf{x}) \in \mathbb{R}^{2\times 2}; \mathbf{x} \in \Omega\}$ with the property that either $\hat{A}_{22}^{pv} \notin M$ or if $\hat{A}_{22}^{pv} \in M$, (i.e., $\hat{A}_{22} = \max_\Omega M$), then for any $\hat{\mathbf{x}} \in \Omega$ such that $\hat{A}_{22} = A_{22}(\hat{\mathbf{x}})$, $\hat{\mathbf{x}} \in \mathbb{R}_+^{2P} \times \{0\}^{2PV}$.

C5 The spectral abscissa of the matrix $\hat{A}_{22}^{pv}$ verifies $\sigma(\hat{A}_{22}^{pv}) \leq 0$ when $\mathcal{R}_0^{(1)} \leq 1$.

The right-hand side of (47) is of class C^1 on the open set $\mathbb{R}_+^{2P} \times \mathbb{R}_+^{2PV}$, so solutions are defined. Solutions in Ω remain in Ω. Furthermore, extending Ω as

$$\Omega_\delta = l\{([\![S_p]\!], [\![L_{pv}]\!], [\![I_{pv}]\!], [\![R_p]\!]) \in \mathbb{R}^{2P(V+1)} :$$
$$N_p = S_P + \sum_{v=1}^{V}(L_{pv} + I_{pv}) + R_p \leq \frac{b_p}{d_p} + \delta; \quad p = 1, \ldots, Pr\},$$

we have that solutions with initial conditions in $\mathbb{R}^{2P(V+1)}$ eventually enter Ω_δ, for any $\delta > 0$. As a consequence, (47) is dissipative and **C1** is satisfied. Then note that in the original form, the model without disease is, for $p = 1, \ldots, P$,

$$\dot{S}_p = b_p - d_p S_p, \tag{49a}$$
$$\dot{R}_p = -d_p R_{pv}. \tag{49b}$$

Thus it is clear that for each $p = 1, \ldots, P$, $S_p(t) \to b_d/d_p$ and $R_p(t) \to 0$ regardless of initial conditions, meaning that condition **C2** holds. Matrix (45) is in block-diagonal form and as a consequence, is block upper triangular. Recall that a matrix is Metzler if its offdiagonal entries are nonnegative, so **C3** holds.

To verify that **C4** holds, remark that for solutions in Ω, the maximal value for a given S_p is attained when $S_p = N_p$, i.e., at the disease-free equilibrium $\mathbf{x}_S^0$. In other words, for $\tilde{\mathbf{x}} \in \mathbb{R}_+^{2P} \times \{0\}^{2PV}$, $\tilde{\mathbf{x}}_S \leq \mathbf{x}_S^0$. Thus, the upper-bound matrix is $\hat{A}_{22} = \hat{A}_{22}(\mathbf{x}_S^0, \mathbf{0}) = \mathbf{G} - \mathbf{W}$. Note that the result can also be formulated using blocks $\hat{A}_{22}^{pv}$ as in (45) and selecting the relevant components in $\mathbf{\Pi}(\mathbf{G} - \mathbf{W})\mathbf{\Pi}^T$, but we do need the form using the unreduced matrix $\hat{A}_{22}$ to show that condition **C5** holds.

Indeed, to show **C5**, return to the unreduced form (48) and note that we have $\sigma(\hat{A}_{22}) = \sigma(\mathbf{G} - \mathbf{W})$, with the matrices as defined in Sect. 2.3 and satisfying the conditions of (van den Driessche and Watmough (2002),Theorem 2). The proof of that theorem establishes that $\mathcal{R}_0 < 1$, i.e., the spectral radius $\rho(\mathbf{G}\mathbf{W}^{-1}) < 1$, is equivalent to the spectral abscissa $\sigma(\mathbf{G} - \mathbf{W}) < 0$. As a consequence, when $\mathcal{R}_0 < 1$, then $\sigma(\hat{A}_{22}) < 0$ and the same is true for each diagonal block $\hat{A}_{22}^{pv}$ in the matrix in normal form (45), since it is similar to (48).

Since conditions **C1**–**C5** are satisfied, the proof is done.

C Proof of Theorem 3

The Jacobian of (15) is the $2PV \times 2PV$ block matrix

$$D\mathbf{F}\left(\mathbf{u}^{\ell}, \mathbf{u}^{i}\right) = \begin{pmatrix} \mathbf{0} & \mathbb{M}_{12} \\ \mathbb{M}_{21} & \mathbb{M}_{22} \end{pmatrix}, \tag{50}$$

where each block has size $PV \times PV$. First,

$$\mathbb{M}_{12} = \mathsf{diag}\left(\left[\!\left[\frac{\varepsilon_{pv}}{\varepsilon_{pv}+d_p}\right]\!\right]\right), \ \mathbb{M}_{22} = \mathsf{diag}\left(\left[\!\left[\frac{\sum_{q=1}^{P} S_q^0 u_{qv}^{\ell}}{\Lambda_{pv}}\right]\!\right]\right).$$

Then, the $PV \times PV$-matrix $\mathbb{M}_{21}$ is itself a block matrix, with each $V \times V$ sized block taking the form, for $p, q \in \{1, \ldots, P\}$,

$$\mathcal{K}_{pq} = S_q^0 \mathsf{diag}\left(\left[\!\left[\frac{\beta_{pqv} u_{pv}^{i}}{\Lambda_{pv}}\right]\!\right]\right).$$

(i) It is clear that (50) is such that if $\mathbf{x}, \mathbf{y} \in [0, 1)^{2PV}$ are such that $\mathbf{x} \leq \mathbf{y}$, one has $D\mathbf{F}(\mathbf{x}) \leq D\mathbf{F}(\mathbf{y})$. Indeed, terms $\mathbf{u}^{\ell}$ and $\mathbf{u}^{i}$ appear as sums in the numerators of the expressions involving them. Furthermore, $\mathbf{F}(\mathbf{0}) > \mathbf{0}$, i.e., it is a nonnegative matrix with some positive entries. This implies that the multitype branching processes are not singular (Berman and Plemmons (January 1979),Theorem 2.3).

(ii) The matrix of first moments is $\mathbb{M} = D\mathbf{F}(\mathbb{1}_{2PV})$, where $\mathbb{1}_{2PV}$ is the unit column vector of size $2PV$. In the transformed matrix (46), diagonal blocks of $\mathbb{M}$ take the form

$$\begin{pmatrix} 0 & \dfrac{\varepsilon_{pv}}{\varepsilon_{pv}+d_p} \\ S_p^0 \dfrac{\beta_{pqv}}{\Lambda_{pv}} & \dfrac{\sum_{q=1}^{P} S_q^0}{\Lambda_{pv}} \end{pmatrix}$$

and are therefore irreducible (and even primitive). Consequently, the matrix of first moments $\mathbb{M}$ is block-primitive.

From (i) and (ii), we conclude that the branching process is positive and regular. As a consequence, applying the (Allen and van den Driessche (May 2013),Threshold Theorem) together with (Harris (1963) ,Theorem 7.1 (Chapter 2))to each of the diagonal blocks in the matrix in normal form (46), gives the threshold behaviour, with existence of a fixed point $(0, 0) < (z_{pv}^{\ell}, z_{pv}^{i}) < (1, 1)$ additionally to $(z_{pv}^{\ell}, z_{pv}^{i}) = (1, 1)$ when the process is supercritical. Putting things together, under the conditions of Theorem 3, there exists an additional fixed point $\mathbf{0} < z < \mathbf{1}$ when $\mathcal{R}_0 > 1$. Then the probability of extinction is given by:

$$\mathbb{P}_{\text{ext}} = \prod_{p=1}^{P} \prod_{v=1}^{V} (z_{pv}^{\ell})^{\ell_{pv0}} (z_{pv}^{i})^{i_{pv0}} \tag{51a}$$

$$\mathbb{P}_{\text{outbreak}} = 1 - \mathbb{P}_{\text{ext}}, \tag{51b}$$

To finish the proof, it is clear that (15a) implies that $z^{\ell}_{pv} = (\varepsilon_{pv} z^{i}_{pv} + d_p)/(\varepsilon_{pv} + d_p)$, where z^{i}_{pv} is the fixed point of (15b). As a consequence, the probabilities in (51) defined for $\mathcal{R}_0^{(1)} > 1$ become those in (16).

D Existence of a mixed equilibrium for (39)

Suppose that the conditions of Theorem 4 are satisfied: $P = V = 2$, virus 2 is at the disease-free equilibrium (DFE), i.e., $L_{12} = L_{22} = I_{12} = I_{22} = 0$ and $\mathcal{R}_{02} < 1$. We seek equilibria of (39) with positive values for $L^{\star}_{11}$, $I^{\star}_{21}$, $I^{\star}_{11}$ and $I^{\star}_{21}$, under the assumption that $\mathcal{R}_{01} > 1$.

Substituting the DFE of species 2 into (39), we obtain from (39c) that

$$S_1^{\star} = \frac{\varepsilon_{11} + d_1}{\beta_{111} I_{11}^{\star} + \beta_{121} I_{21}^{\star}} L_{11}^{\star}, \quad S_2^{\star} = \frac{\varepsilon_{21} + d_2}{\beta_{211} I_{11}^{\star} + \beta_{221} I_{21}^{\star}} L_{21}^{\star},$$

while (39e) gives

$$L_{11}^{\star} = \frac{\gamma_{11} + d_1}{\varepsilon_{11}} I_{11}^{\star}, \quad L_{21}^{\star} = \frac{\gamma_{21} + d_2}{\varepsilon_{21}} I_{21}^{\star}$$

and, finally, from (39f),

$$R_1^{\star} = \frac{\gamma_{11}}{d_1} I_{11}^{\star}, \quad R_2^{\star} = \frac{\gamma_{21}}{d_2} I_{21}^{\star}.$$

Since the total population of each species is governed, for $i = 1, 2$, by $\dot{N}_i = b_i - d_i N_i$, at an equilibrium, $b_i - d_i N_i^{\star} = 0$ and thus, when (39) is at an equilibrium with virus 2 at the DFE, one has

$$b_1 - d_1 \left(S_1^{\star} + L_{11}^{\star} + I_{11}^{\star} + R_1^{\star}\right) = 0 \quad \text{and} \quad b_2 - d_2 \left(S_2^{\star} + L_{21}^{\star} + I_{21}^{\star} + R_2^{\star}\right) = 0.$$

Expressing all terms as functions of I_{i1}, $i = 1, 2$, and using the expressions of S_1, L_{11}, R_1, S_2, L_{21} and R_2 gives

$$\beta_{111}(I_{11}^{\star})^2 - \left[d_1 (\mathcal{R}_{01} - 1) - \beta_{121} I_{21}^{\star}\right] I_{11}^{\star} - \frac{\beta_{121}}{\beta_{111}} d_1 \mathcal{R}_{01} I_{21}^{\star} = 0, \tag{52a}$$

$$\beta_{221}(I_{21}^{\star})^2 - \left[d_2 (\mathcal{R}_{02} - 1) - \beta_{211} I_{11}^{\star}\right] I_{21}^{\star} - \frac{\beta_{211}}{\beta_{221}} d_2 \mathcal{R}_{02} I_{11}^{\star} = 0. \tag{52b}$$

To simplify computations, let us denote $x = I_{11}^{\star}$ and $y = I_{21}^{\star}$. Then (52) can be written as

$$\Gamma_1(x, y) := \beta_{111} x^2 + \beta_{121} xy - d_1 (\mathcal{R}_{01} - 1)\, x - \frac{\beta_{121}}{\beta_{111}} d_1 \mathcal{R}_{01} y = 0, \tag{53a}$$

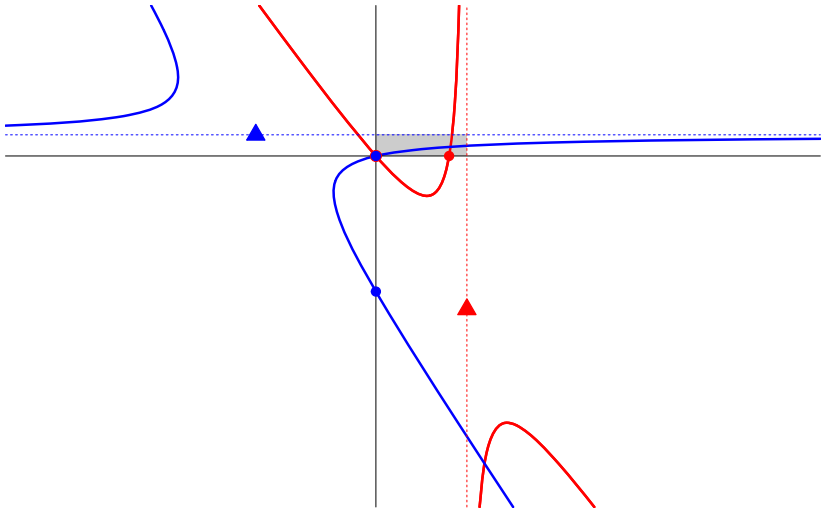

Fig. 8 Situation leading to the existence of a mixed equilibrium. Red curve: Γ_1. Blue curve: Γ_2. The centres of the hyperbolas are shown as triangles of corresponding colours, as are the vertical and horizontal asymptotes relevant to the problem. The shaded box shows the possible range of values of the endemic component of the mixed equilibrium

$$\Gamma_2(x, y) := \beta_{211}xy + \beta_{221}y^2 - \frac{\beta_{211}}{\beta_{221}}d_2\mathcal{R}_{02}x - d_2\left(\mathcal{R}_{02} - 1\right)y = 0. \tag{53b}$$

Both Γ_1 and Γ_2 are conic sections. Their discriminants $-\beta_{121}^2$ and $-\beta_{211}^2$ are both negative, hence they are both hyperbolas. As (53a) has no second degree y monomial, one of its asymptotes is vertical. Likewise, since (53b) has no second degree x monomial, one of its asymptotes is horizontal. If both of these asymptotes intersect the positive (or first) quadrant $Q_1 = \mathbb{R}_+ \times \mathbb{R}_+$, then Γ_1 and Γ_2 intersect a single time there. The situation is shown in Figs. 8 and 9.

Let us show that this is indeed the case. There are two ingredients:

1. The curves Γ_1 and Γ_2 intersect Q_1.
2. The vertical asymptote of Γ_1 and the horizontal asymptote of Γ_2 intersect Q_1.

First, note that the point of intersection $(x, y) = (0, 0)$ is obvious since neither (53a) nor (53b) have terms of degree 0. Now consider the x- and y-intercepts of Γ_1 and Γ_2. For Γ_1, x-intercepts satisfy

$$\Gamma_1(x, 0) = \left(\beta_{111}x - d_1(\mathcal{R}_{01} - 1)\right)x,$$

i.e., $x = 0$ and $x = d_1(\mathcal{R}_{01} - 1)/\beta_{111} > 0$ by the assumption $\mathcal{R}_{01} > 1$. For y-intercepts,

$$\Gamma_1(0, y) = -\frac{\beta_{121}}{\beta_{111}}d_1\mathcal{R}_{01}y,$$

i.e., Γ_1 intercepts the y-axis only at the origin. For Γ_2, x-intercepts are given by

$$\Gamma_2(x,0) = -\frac{\beta_{211}}{\beta_{221}} d_2 \mathcal{R}_{02} x,$$

giving only the origin as x-intercept, while y-intercepts are given by

$$\Gamma_2(0,y) = (\beta_{221} y - d_2(\mathcal{R}_{02} - 1))\, y,$$

i.e., y-intercepts are $y = 0$ and $y = d_2(\mathcal{R}_{02} - 1)/\beta_{221} < 0$ by assumption.

We can therefore establish that Γ_1 and Γ_2 intersect Q_1. Indeed, from the gradients $\nabla\Gamma_1(x,y)$ and $\nabla\Gamma_2(x,y)$, we deduce that vectors tangent to Γ_1 and Γ_2 are

$$T_1(x,y) = \left(\beta_{121}x - \frac{\beta_{121}}{\beta_{111}} d_1\mathcal{R}_{01}, d_1(\mathcal{R}_{01}-1) - 2\beta_{111}x - \beta_{121}y\right),$$
$$T_2(x,y)\left(2\beta_{221}y + \beta_{211}x - d_2(\mathcal{R}_{02}-1), \frac{\beta_{211}}{\beta_{221}} d_2\mathcal{R}_{02} - \beta_{211}y\right).$$

At the origin, $T_1(0,0) = (-\beta_{121}d_1\mathcal{R}_{01}/\beta_{111}, d_1(\mathcal{R}_{01}-1))$ has signs $(-,+)$. This means that Γ_1 "moves" through origin from the second quadrant $Q_2 = \mathbb{R}_- \times \mathbb{R}_+$ when $x < 0$ to the fourth quadrant $Q_4 = \mathbb{R}_+ \times \mathbb{R}_-$ when $x > 0$. On the other hand, $T_2(0,0) = (-d_2(\mathcal{R}_{02}-1), \beta_{211}d_2\mathcal{R}_{02}/\beta_{221})$ has signs $(+,+)$, implying that left of the y-axis, Γ_2 is in the third quadrant $Q_3 = \mathbb{R}_- \times \mathbb{R}_-$, while it is in Q_1 when $x > 0$.

It remains to show that the vertical and horizontal asymptotes of Γ_1 and Γ_2, respectively, intersect the positive quadrant Q_1.

The centre of Γ_1 is $(d_1\mathcal{R}_{01}/\beta_{111}, -d_1(\mathcal{R}_{01}+1)/\beta_{121}) \in Q_4$ (red triangle in Fig. 8). Since Γ_1 intersects Q_2, the asymptote to $\Gamma_1 \cap Q_2$ has negative slope. It follows that the vertical asymptote to Γ_1 is the one to $\Gamma_1 \cap Q_1$ and therefore, intersects Q_1. Reasoning similarly, observe that since the centre $(-d_2(\mathcal{R}_{02}+1)/\beta_{211}, d_2\mathcal{R}_{02}/\beta_{221})$ of Γ_2 lies in Q_2 (blue triangle in Fig. 8) and Γ_2 intersects Q_4, the asymptote to $\Gamma_2 \cap Q_4$ has negative slope and that to the part of $\Gamma_2 \cap Q_1$ is horizontal.

As a consequence, there is a point in the interior of the positive quadrant Q_1 where Γ_1 intersects Γ_2. More precisely, remark that since the centres of the hyperbola lie on the vertical and horizontal asymptotes, respectively, the x-coordinate of the point of intersection cannot be larger that the x-component of the centre of Γ_1 and its y-coordinate cannot exceed the y-component of the centre of Γ_2. This means that the endemic equilibrium belongs to the box

$$\left(0, \frac{d_1\mathcal{R}_{01}}{\beta_{111}}\right] \times \left(0, \frac{d_2\mathcal{R}_{02}}{\beta_{221}}\right] \tag{54}$$

shown shaded in Figs. 8 and 9.

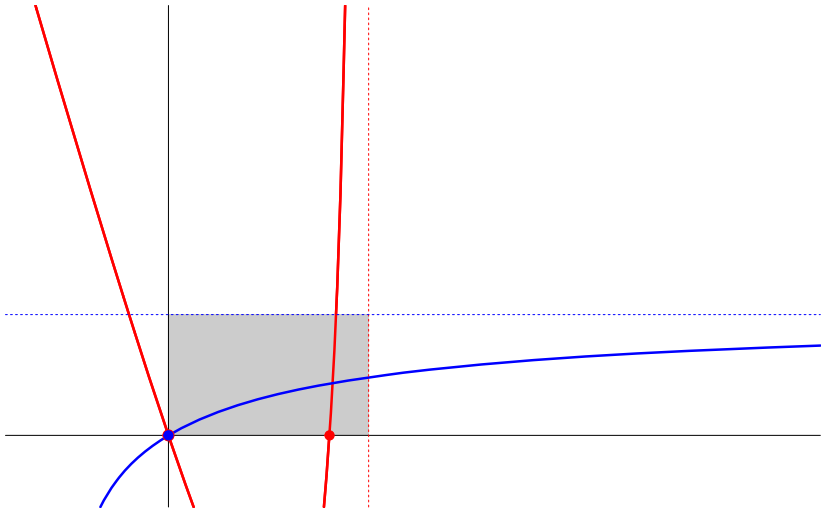

Fig. 9 Situation leading to the existence of a mixed equilibrium. Zoom on Fig. 8 focusing on the positive quadrant. Γ_1 and its related features is shown in red, while Γ_2 is in blue (Color figure online)

Acknowledgements The authors thank Sharon Clouthier, Karen Dunmall and Collin Ghallagher, from the Freshwater Institute (Department of Fisheries and Oceans Canada, Winnipeg) for initiating the project and helpful discussions. They also thank anonymous reviewers whose comments greatly improved the manuscript. JA acknowledges support from NSERC through the Discovery Grants program.
CD was supported in part by a 2024/2025 Maud Menten Institute (MMI) Research Accelerator Award. CD thanks the MMI Community and the MMI Co-Directors for their support. JA was supported in part by an NSERC Discovery Grant.

References

Alaska (2024) Department of Fish and Game. Pacific herring (Clupea pallasii), n.d. Accessed on February 2
Allen L.J.S (2010). An Introduction to Stochastic Processes with Applications to Biology. CRC Press,
Allen LJS, van den Driessche P (2013) Relations between deterministic and stochastic thresholds for disease extinction in continuous- and discrete-time infectious disease models. Mathematical Biosciences 243(1):99–108
Almarashi RM, McCluskey CC (2019) The effect of immigration of infectives on disease-free equilibria. Journal of Mathematical Biology 79:1015–1028
Arechavala-Lopez P, Sanchez-Jerez P, Bayle-Sempere JT, Uglem I, Mladineo I (2013) Reared fish, farmed escapees and wild fish stocks-a triangle of pathogen transmission of concern to mediterranean aquaculture management. Aquaculture Environment Interactions 3(2):153–161
Arino J, Bajeux N, Portet S, Watmough J (2020) Quarantine and the risk of COVID-19 importation. Epidemiology & Infection 148:e298
Arino J, Boëlle P-Y, Milliken EM, Portet S (2021) Risk of COVID-19 variant importation - How useful are travel control measures? Infectious Disease Modelling 6:875–897
Arino J, Davis JR, Hartley D, Jordan R, Miller J, van den Driessche P (2005) A multi-species epidemic model with spatial migration. Mathematical Medicine and Biology 22(2):129–142
Arino J, Milliken E.M (2022). Effect of mobility on the stochastic phase of an epidemic. Bulleting of Mathematical Biology, 84,
Athreya K.B, Ney P.E (1972). Branching Processes. Springer,
Atkins KE, Travis JMJ (2010) Local adaptation and the evolution of species-ranges under climate change. Journal of Theoretical Biology 266(3):449–457

Batts W.N, Lovy J, Getchell R.G, Faisal M, Standish I, Warg J.V, Phelps N.B.D, Glenney G, Winton J.R(2020) . Viral Hemorrhagic Septicemia. USGS Western Fisheries Research Center,

Bergh Ø, Børsheim KY, Bratbak G, Heldal M (1989) High abundance of viruses found in aquatic environments. Nature 340(6233):467–468

Berman A, Plemmons RJ (1979) Nonnegative matrices in the mathematical sciences. Academic Press, New York

Carlson CJ, Albery GF, Merow C, Trisos CH, Zipfel CM, Eskew EA, Olival KJ, Ross N, Bansal S (2022) Climate change increases cross-species viral transmission risk. Nature 607(7919):555–562

Dixon P, Paley R, Alegria-Moran R, Oidtmann B (2016) Epidemiological characteristics of infectious hematopoietic necrosis virus (IHNV): a review. Veterinary Research 47(1):1–26

Ellwanger JH, Chies JAB (2021) Zoonotic spillover: Understanding basic aspects for better prevention. Genetics and Molecular Biology 44(1 Suppl 1):e20200355

Foott JS, Free D, McDowell T, Arkush KD, Hedrick RP (2006) Infectious Hematopoietic Necrosis Virus transmission and disease among juvenile Chinook salmon exposed in culture compared to environmentally relevant conditions. San Francisco Estuary and Watershed Science 4(1):2

Fowler AC (2021) Atto-foxes and other minutiae. Bulletin of Mathematical Biology 83(10):104

Gagné N, MacKinnon A-M, Boston L, Souter B, Cook-Versloot M, Griffiths S, Olivier G (2007) Isolation of Viral Haemorrhagic Septicaemia Virus from Mummichog, Stickleback, Striped bass and Brown trout in eastern Canada. Journal of Fish Diseases 30:213–223

Garver KA, Hawley LM (2021) Characterization of viral haemorrhagic septicaemia virus (VHSV) to inform pathogen transfer risk assessments in British Columbia. Technical Report DFO Can. Sci. Advis. Sec. Res. Doc, Fisheries and Oceans Canada, Canadian Science Advisory Secretariat

Harris TE (1963) The Theory of Branching Processes, vol 119. Grundlehren der mathematischen Wissenschaften. Springer, Berlin, Heidelberg

Heathcote CR (1965) A branching process allowing immigration. Journal of the Royal Statistical Society Series B: Statistical Methodology 27(1):138–143

Hershberger PK, Gregg JL, Grady CA, Collins RM, Winton JR (2010) Susceptibility of three stocks of Pacific herring to Viral Hemorrhagic Septicemia. Journal of Aquatic Animal Health 22(1):1–7

Johansen L-H, Jensen I, Mikkelsen H, Bjørn P-A, Jansen PA, Bergh Ø (2011) Disease interaction and pathogens exchange between wild and farmed fish populations with special reference to norway. Aquaculture 315(3–4):167–186

Kamgang J-C, Sallet G (2008) Computation of threshold conditions for epidemiological models and global stability of the disease-free equilibrium (DFE). Mathematical Biosciences 213(1):1–12

Karvonen Anssi, Jokela Jukka, Laine Anna-Liisa (2019) Importance of sequence and timing in parasite coinfections. Trends in parasitology 35(2):109–118

Kirkpatrick M, Barton NH (1997) Evolution of a species' range. The American Naturalist 150(1):1–23

Klein EY, Monteforte B, Gupta A, Jiang W, May L, Hsieh YH, Dugas A (2016) The frequency of influenza and bacterial coinfection: a systematic review and meta-analysis. Influenza and other respiratory viruses 10(5):394–403

Kocan RM, Hershberger PK, Elder NE, Winton JR (2001) Epidemiology of viral hemorrhagic septicemia among juvenile Pacific herring and Pacific sand lances in Puget Sound. Washington. Journal of Aquatic Animal Health 13:77–85

Kotob MH, Menanteau-Ledouble S, Kumar G, Abdelzaher M, El-Matbouli M (2017) The impact of co-infections on fish: a review. Veterinary research 47:1–12

Krammer F (2019) The human antibody response to influenza a virus infection and vaccination. Nature Reviews Immunology 19(6):383–397

Krkosek M, Ford JS, Morton A, Lele S, Myers RA, Lewis MA (2007) Declining wild salmon populations in relation to parasites from farm salmon. Science 318(5857):1772–1775

LaPatra SE, Barone L, Jones GR, Zon LI (2000) Effects of infectious Hematopoietic Necrosis Virus and infectious Pancreatic Necrosis Virus infection on hematopoietic precursors of the zebrafish. Blood Cells, Molecules, and Diseases 26(5):445–452

Meadows AJ, Stephenson N, Madhav NK, Oppenheim B (2023) Historical trends demonstrate a pattern of increasingly frequent and severe spillover events of high-consequence zoonotic viruses. BMJ Global Health 8(11):e012026

Meyers TR, Short S, Lipson K, Batts WN, Winton JR, Wilcock J, Brown E (1994) Association of viral hemorrhagic septicemia virus with epizootic hemorrhages of the skin in Pacific herring Clupea harengus

pallasi from Prince William Sound and Kodiak Island, Alaska, USA. Diseases of Aquatic Organisms 19:27–37
Meyers TR, Sullivan J, Emmenegger E, Follett J, Short S, Batts WN, Winton JR (1992) Identification of viral hemorrhagic septicemia virus isolated from Pacific cod Gadus macrocephalus in Prince William Sound, Alaska, USA. Diseases of Aquatic Organisms 12:167–175
Meyers TR, Winton JR (1995) Viral Hemorrhagic Septicemia Virus in North America. Annual Review of Fish Diseases 5:3–24
Mitro M.G, White A.L (2008). Viral Hemorrhagic Septicemia and Freshwater Fisheries: The State of the Science. Technical Bulletin No. 196 Department of Natural Resources,
National Oceanic and Atmospheric Administration (NOAA). Chum salmon. NOAA Fisheries website, (2023a). Last updated on 12/22/2023
National Oceanic and Atmospheric Administration (NOAA). Sockeye salmon. NOAA Fisheries website, (2023b). Last updated on 12/22/2023
Ord W.M, Le Berre M, de Kinkelin P (1976). Viral Hemorrhagic Septicemia: Comparative susceptibility of Rainbow trout (salmo gairdneri) and Hybrids (s. gairdneri × oncorhynchus kisutch) to experimental infection. Journal of the Fisheries Research Board of Canada, 33(5):1205–1208,
Pakes AG (1971) Branching processes with immigration. Journal of Applied Probability 8(1):32–42
Parmesan C (2006) Ecological and evolutionary responses to recent climate change. Annual Review of Ecology, Evolution, and Systematics 37:637–669
Phillips BL, Brown GP, Shine R (2010) Life-history evolution in range-shifting populations. Ecology 91(6):1617–1627
Rucker RR, Whipple WJ, Parvin JR, Evans CA (1953) A contagious disease of salmon possibly of virus origin. Fishery Bulletin of the Fish and Wildlife Service 54:35–46
Sánchez CA, Li H, Phelps KL, Zambrana-Torrelio C, Wang L-F, Zhou P, Shi Z-L, Olival KJ, Daszak P (2022) A strategy to assess spillover risk of bat SARS-related coronaviruses in Southeast Asia. Nature Communications 13(1):4380
Sexton JP, McIntyre PJ, Angert AL, Rice KJ (2009) Evolution and ecology of species range limits. Annual Review of Ecology, Evolution, and Systematics 40:415–436
Spickler A.R (2024). Infectious hematopoietic necrosis, 2007. http://www.cfsph.iastate.edu/DiseaseInfo/factsheets.php, Retrieved on January 19,
Stokesbury K D E, Kirsch J, Patrick E V, L/Norcross B (2002) Natural mortality estimates of juvenile Pacific herring (Clupea pallasi) in Prince William Soun. Alaska. Canadian Journal of Fisheries and Aquatic Sciences 59(3):424–433
Suttle CA (2007) Marine viruses-major players in the global ecosystem. Nature Reviews Microbiology 5(10):801–812
Takano R, Mori K, Nishizawa T, Arimoto M, Muroga K (2001) Isolation of viruses from wild Japanese flounder. Paralichthys olivaceus. Fish Pathology 36:153–160
van den Driessche P, Watmough J (2002) Reproduction numbers and sub-threshold endemic equilibria for compartmental models of disease transmission. Mathematical Biosciences 180(1):29–48
Wommack KE, Colwell RR (2000) Virioplankton: viruses in aquatic ecosystems. Microbiology and Molecular Biology Reviews 64(1):69–114
Wyn-Jones AP, Sellwood J (2001) Enteric viruses in the aquatic environment. Journal of Applied Microbiology 91(6):945–962
Yong CY, Ong HK, Tang HC, Yeap SK, Omar AR, Ho KL, Tan WS (2019) Infectious Hematopoietic Necrosis Virus: Advances in diagnosis and vaccine development. PeerJ 7:e7151